

POLITECNICO DI MILANO
School of Industrial and Information Engineering
Department of Chemistry, Materials,
and Chemical Engineering "Giulio Natta"
Master of Science in Chemical Engineering



POLITECNICO
MILANO 1863

**Jet fuel surrogates formulation
and metamodeling of
fuel mixtures properties**

Supervisor:

Prof. Marco Mehl

Co-supervisor:

Prof. Alberto Cuoci

Candidate:

Simone Pertesana

941135

Academic Year 2020-2021

Abstract

The aviation is a sector where technologies alternative to fossil fuels are not expected to become available in the near future. For this reason the efficient exploitation of the currently available resources is mandatory. However, the development of new engines and new fuels is characterized by a large number of tests (that can be expensive), requiring a long bureaucratic procedure.

Due to these aspects and to ensure the reproducibility, the preliminary tests are carried out using surrogates of the fuels: mixtures with simple and defined composition whose properties are similar to the ones of the fuel of interest.

The object of this thesis work is the development of a `Matlab`[®] framework to ease the surrogates evaluation and screening procedures. The resulting code requires as input only the properties of the real fuel and a palette of chemical compounds, among which it will choose the ones to formulate the surrogate.

These properties have been implemented: density, molecular weight, H/C ratio, cetane number, viscosity, sooting index, distillation curve, ignition delay times and laminar burning velocities.

Mixing rules for the last two properties were not available, so dedicated models have been developed exploiting heavy numerical simulations carried out using the `OpenSMOKE++` Suite. A Kriging model is used to describe ignition delay times, while a polynomial one is built to describe laminar burning velocities. These approximate mixing rules allows a quick estimation compatible

with the iterative formulation procedure.

The problem of the formulation of a mixture whose properties are as similar as possible to a given target is transposed to the minimization of properties differences: this allows to describe the formulation as an optimization. A study about the possibility to use only a small set of known properties and the importance of each property is carried out.

The framework allows an efficient surrogate formulation with a small data supply required from the user. Its validity is confirmed by comparison between the formulated surrogates for a real fuel and surrogates already available in the scientific literature.

Sommario

L'aviazione è un settore in cui è difficile immaginare lo sviluppo di tecnologie alternative ai combustibili fossili nel breve periodo. È quindi necessario sfruttare al meglio le risorse disponibili. Tuttavia, lo sviluppo di nuovi motori e carburanti è caratterizzato da numerosi test (potenzialmente costosi) e lunghi iter burocratici.

Per questo e per garantire la riproducibilità, i test preliminari vengono effettuati utilizzando surrogati dei combustibili: miscele di composizione semplice e definita le cui proprietà siano simili a quelle del combustibile considerato.

L'obiettivo di questa tesi è lo sviluppo di un framework `Matlab`[®] per semplificare le procedure di valutazione e selezione dei surrogati, richiedendo in input solo le proprietà del carburante e un insieme di composti tra cui vengono scelte le specie per costruire il surrogato.

Sono state considerate le seguenti proprietà: densità, peso molecolare, rapporto H/C, numero di cetano, viscosità, indice di sooting, curva di distillazione, tempi di ignizione e velocità laminari di fiamma.

Data la mancanza di regole di miscelazione per le ultime due, sono stati sviluppati modelli dedicati sfruttando simulazioni, computazionalmente costose, effettuate tramite la `OpenSMOKE++` Suite. Un modello di Kriging è stato utilizzato per descrivere i tempi di ignizione, mentre uno polinomiale è stato usato per le velocità laminari di fiamma. Questi modelli approssimati per-

mettono una stima rapida di tali proprietà, compatibile con la procedura iterativa di formulazione.

Il problema della formulazione di una miscela con proprietà il più simili possibile ad un dato target si rispecchia nella minimizzazione delle differenze di proprietà tra target e surrogato: è possibile descrivere la formulazione come un'ottimizzazione. È stata studiata la possibilità di utilizzare solo alcune delle proprietà note e l'importanza di ciascuna proprietà.

Il framework consente la formulazione efficiente di un surrogato con pochi dati richiesti all'utente. La sua validità è confermata confrontando i surrogati formulati per un carburante con surrogati disponibili nella letteratura scientifica.

Contents

1	Introduction	17
1.1	An overview of the energetic scenario	17
1.2	The transportation sector	20
1.3	Jet fuels	22
1.3.1	Jet fuel standards	22
1.3.2	Jet fuels requirements	23
1.3.3	Approval of a new jet fuel	26
1.4	Aim of this work	27
2	Fuel properties and optimization algorithms	30
2.1	Chemico-physical properties	30
2.2	Optimization algorithms	35
2.2.1	Introduction to constrained optimization	35
2.2.2	Genetic algorithm	36
2.2.3	Particle swarm algorithm	37
2.2.4	Pattern search algorithms	38

Contents

2.2.5	fmincon	38
2.2.6	Summary of optimization algorithms	39
2.3	Root-finding algorithms	39
2.3.1	Secant method	39
3	Derivation of a metamodel for ignition delay times	41
3.1	Species and operating conditions	43
3.2	Simulation of IDTs	44
3.2.1	The use of OpenSMOKE++ Suite	44
3.2.2	Outliers handling	45
3.3	Data preprocessing	46
3.4	Kriging models	47
3.4.1	Estimation of parameters	50
3.4.2	Addition of points	51
3.5	Results	51
3.6	Model verification	53
3.7	Summary	57
4	Derivation of a metamodel for laminar burning velocities	58
4.1	Simulation of LBV	59
4.2	Polynomial models	60
4.3	Parameter estimation	62
4.4	Obtained parameters	65
4.5	Model verification	67

4.6 Summary	72
5 Development of an optimization strategy for surrogates for- mulation	73
5.1 The objective function	74
5.2 The optimization algorithm	75
5.3 Validation of the optimization strategy	78
5.4 Selection of properties to be optimized	83
5.4.1 Selection of two basic properties	84
5.4.2 Addition of a third property	85
5.4.3 Addition of a fourth property	87
5.4.4 Analysis of results	89
5.5 Selection of optimization weights	90
5.6 Summary	92
6 Application to real fuels	93
6.1 A surrogate for POSF-4658	94
6.2 Comparison with surrogates available in the literature	99
6.3 A surrogate for Jet A-1	102
6.4 Summary	106
7 Conclusions and future developments	107
A Kriging model for IDT	110

Contents

B Data about the optimizer behavior respect to the optimized properties	113
List of symbols and acronyms	116
Bibliography	120

List of Figures

1.1	World primary energy consumption by source (1)	18
1.2	Global greenhouse gas emissions (2)	18
1.3	Energy consumption by sector, OECD, 1971-2018 (3)	19
1.4	Energy consumption by sector and source, OECD, 2018 (4)	20
1.5	Fuel consumption in transport - European Union (6)	21
1.6	Greenhouse gas emissions from transport in European Union, 2014 (7)	21
1.7	Overview Fuel and Additive Approval Process (16).	26
3.1	Example of IDT curve	42
3.2	Considered species for the surrogate formulation	43
3.3	Comparison of full-factorial (structured) and latin hypercube methods to choose sampling points in a 3D space	48
3.4	Trends of ϑ parameters with respect to pressure	52
3.5	Validation of 12 sets of 500 points with the 6 component Kri- ging model	54

List of Figures

3.6	IDT curves for target and optimized mixtures	57
4.1	Example of LBV curve	59
4.2	LBV curves for pure components	63
4.3	Obtained parameters for LBV models #1 - #3, in absolute value	66
4.4	Validation of LBV models with a random mixture	68
4.5	LBV curves for target and optimized mixtures	71
5.1	Representation of the objective function in the 4-dimensional space	80
5.2	Representation of the objective function in the 6-dimensional space	81
5.3	Properties of the surrogate for test mix #2 obtained optimiz- ing ρ and H/C	84
5.4	Comparison of ε between surrogates obtained by optimizing 2 and 3 properties	86
5.5	Properties of the surrogate for test mix #2 obtained optimiz- ing ρ , H/C and CN	86
5.6	ε on each property (on the columns) for each set of properties optimized (on the rows) - reported as average on the three test mixtures. An additional data on composition is reported as average Δx on families (test #3 is not considered in this last column as the species palette is smaller than the target).	88

6.1	Properties of POSF-4658 surrogates	96
6.2	Ignition delay times and laminar burning velocities of POSF-4658 (35 , 40) and of derived surrogates	98
6.3	Molar composition of POSF-4658 surrogates by families	99
6.4	Comparison of POSF-4658 surrogates' curves	100
6.5	Molar composition of Jet A-1 surrogates by families	103
6.6	Properties of Jet A-1 surrogates	104
6.7	Ignition delay times and laminar burning velocities of Jet A-1 (43 , 44) and of surrogates	105

List of Tables

1.1	Jet fuel properties	23
2.1	Numerical values of the considered properties	34
3.1	Ranges of conditions considered for IDT metamodel	44
3.2	Upper and lower limits for parameters ϑ and λ	51
3.3	Values of R^2 computed on subsets of validation simulations, each obtained by bounding one variable	55
3.4	Compositions of some test mixtures and their optimized sur- rogates	56
4.1	Simulation conditions for laminar burning velocities	62
4.2	Boundaries for LBV model parameters	64
4.3	Obtained parameters for LBV model #1 - #3	65
4.4	Obtained parameters for LBV model #4	67
4.5	R^2 values for the validation mixtures	69
4.6	Comparison of three 'target' mixtures and the mixtures ob- tained with models so that the LBV curve is well fitted	70

5.1	Comparison of different optimization routines and routines combinations	77
5.2	Weights used in the objective function	78
5.3	Test #1 results - Mixtures	79
5.4	Test #1 results - Objective function	79
5.5	Test #2 results - Mixtures	80
5.6	Test #2 results - Objective function	81
5.7	Test #3 results - Mixtures	82
5.8	Test #3 results - Objective function	83
5.9	Proposed weights to be used in the objective function	91
5.10	Composition of the objective function using the proposed weight set	91
6.1	Properties of POSF-4658 fuel	94
6.2	Composition of POSF-4658 surrogates (one per column)	97
6.3	Comparison of POSF-4658 surrogates' properties	100
6.4	Properties of Jet A-1 - Source (42)	102
6.5	Composition of Jet A-1 surrogates (one per column)	103

List of Tables

Chapter 1

Introduction

This chapter introduces the context and the scope of this work: the environmental reasons of the choice of aviation sector and jet fuels are reported. Also, a brief summary of what a jet fuel is, its properties and the necessity of surrogates is presented here.

1.1 An overview of the energetic scenario

Energy and its use are some of the biggest challenges of this time.

The world's energy consumption has grown for the last years and the available forecasts predict that it will keep growing in the next decades.

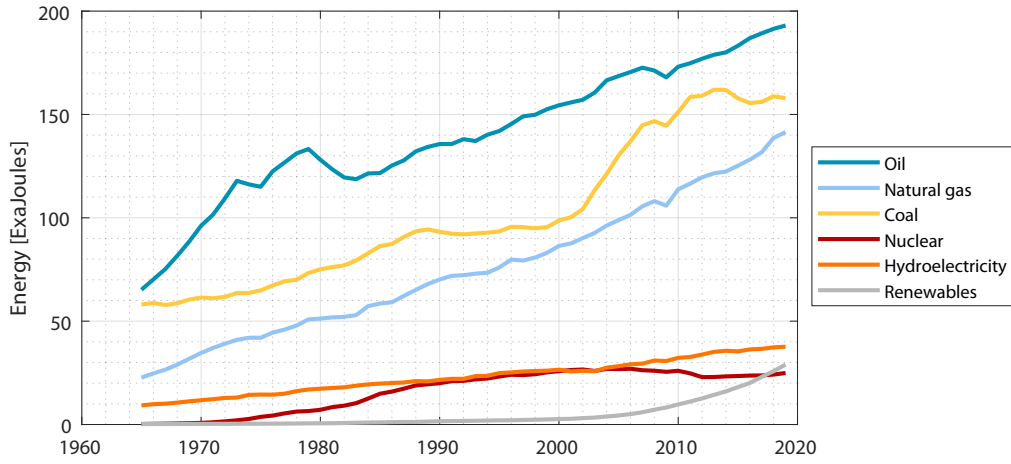


Figure 1.1: World primary energy consumption by source (1)

The energy production from fossil fuels (that still represents a relevant fraction of the total, as reported in Figure 1.1) has however significant drawbacks in terms of environmental impact of its emissions. The main issues related to such emissions are the greenhouse effect (the CO_2 derived from fossil fuels

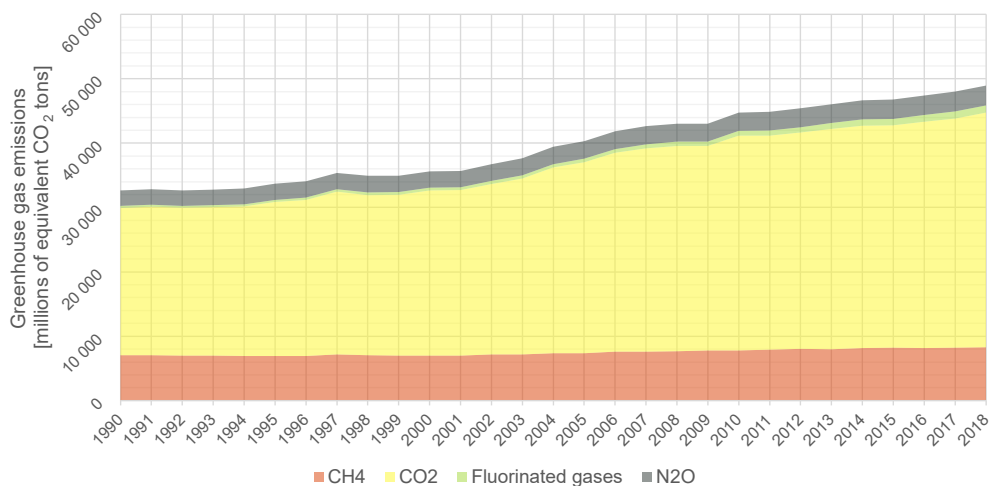


Figure 1.2: Global greenhouse gas emissions (2)

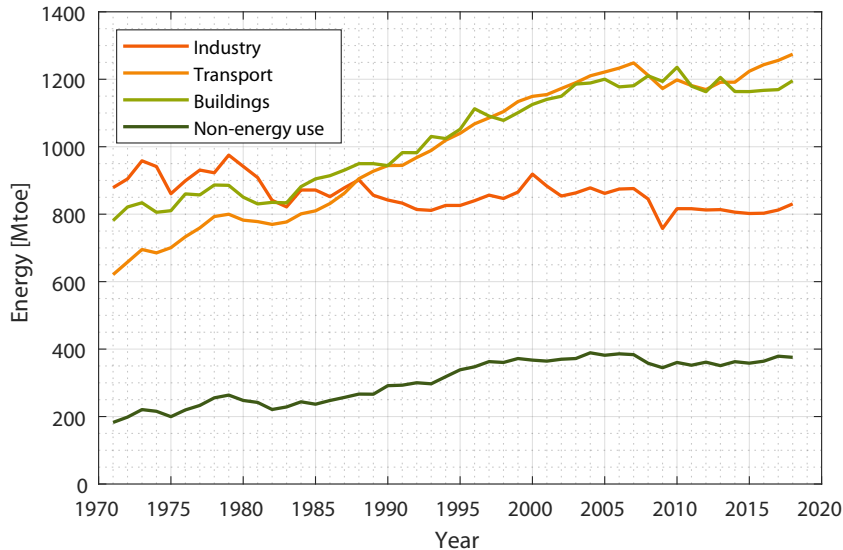


Figure 1.3: Energy consumption by sector, OECD, 1971-2018 (3)

combustion is the major responsible for greenhouse effect, as shown in Figure 1.2), that has climate related consequences and the polluting effect of several combustion byproducts.

In particular, the transport sector accounts for the largest part of energy consumption (Figure 1.3) and, compared to industrial, commercial and domestic sectors, is the one that exploits the most fossil fuels (more than 90% of energy consumed by transports comes from fossil sources, as reported in Figure 1.4).

If some techniques are available or under study to reduce the impact of fossil fuel combustion, many of them (e.g. downstream treatments, carbon capture systems...) are developed for fixed applications, and are not easy to be implemented in transportation, where space occupation must be reduced to lowest terms and weight has a major impact on vehicles efficiency.

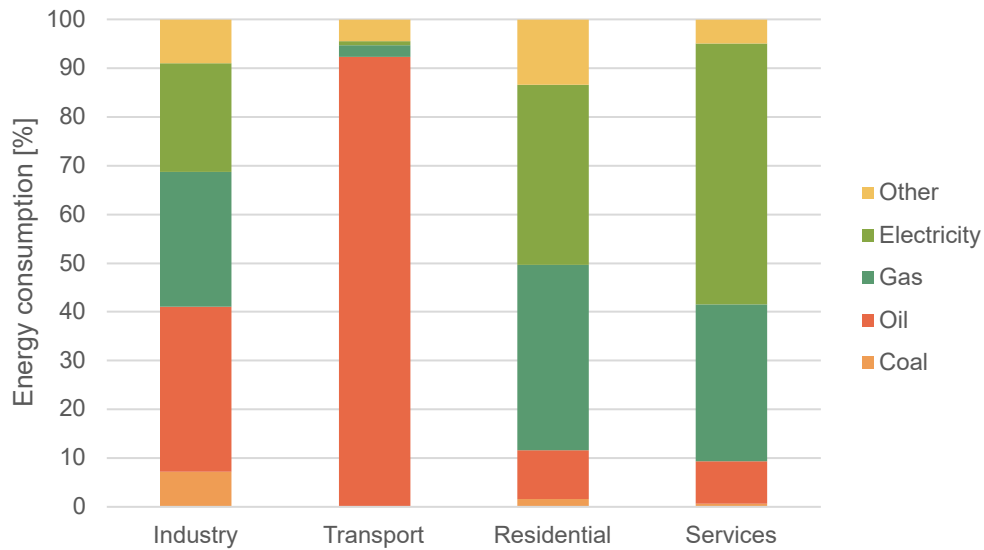


Figure 1.4: Energy consumption by sector and source, OECD, 2018 (4)

Since transportation is the sector where challenges revealed to be the hardest (5), this work will be based around this sector.

1.2 The transportation sector

Focusing now on the transportation sector, it's possible to see that road vehicles contribute the most to greenhouse effect (Figures 1.5 - 1.6): however, recent trends show the approach to new environmentally-friendly technologies, like the use of hydrogen or methane as fuels, or electric vehicles. So, it is reasonable to expect that the impact of road transportation will decrease in the near future.

Rail transport can be electrified without too much expenses, shifting the problem of energy production to power plants, where countermeasures to

1.2. The transportation sector

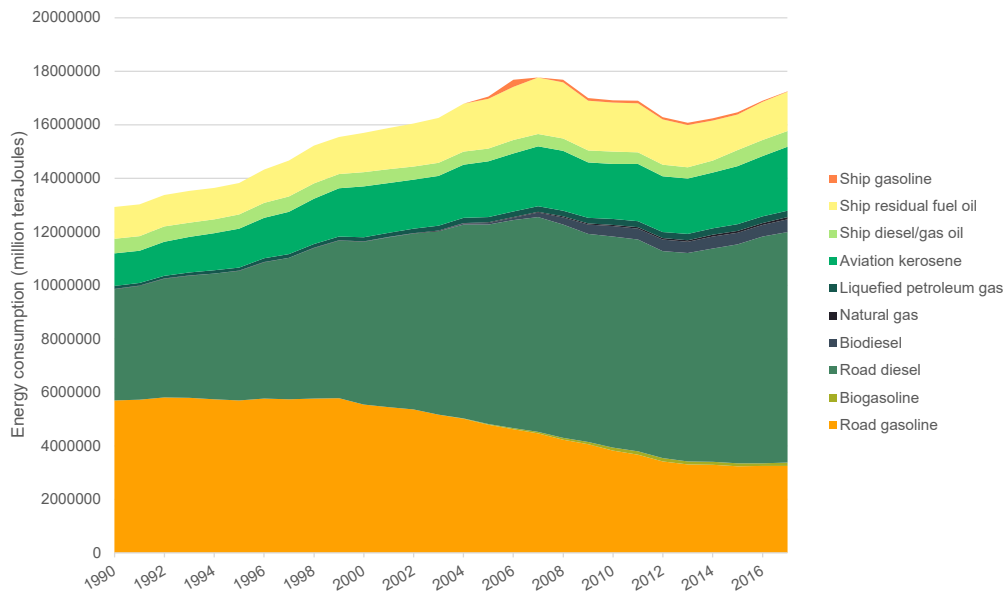


Figure 1.5: Fuel consumption in transport - European Union (6)

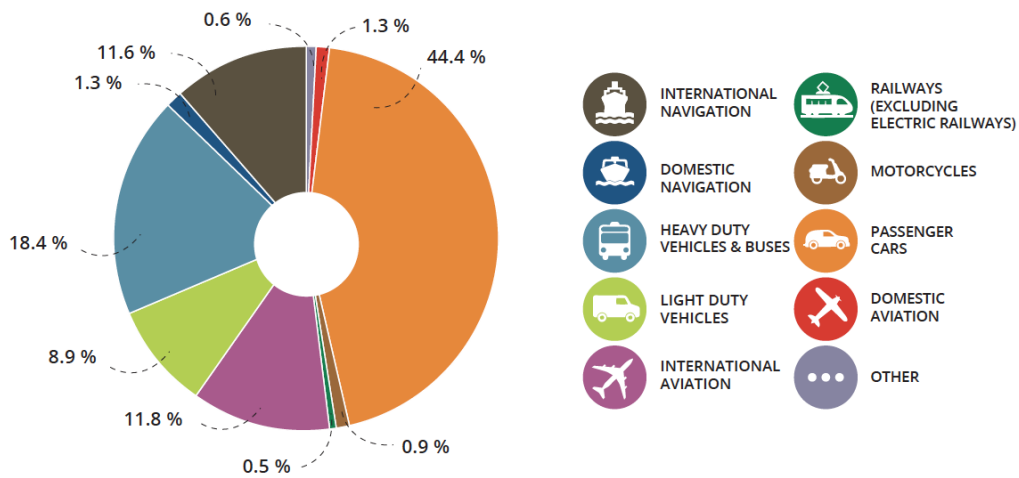


Figure 1.6: Greenhouse gas emissions from transport in European Union, 2014 (7)

pollution and greenhouse effects are easier to be implemented (if the plant doesn't use a renewable energy source itself).

The most problematic sectors are the aviation and the navigation, where al-

alternatives to internal combustion engines can't be expected to become available in the near future. Being the number of air passengers expected to increase (8), this work is focused on aviation, in particular on jet fuels.

1.3 Jet fuels

Jet fuels - ignitable mixtures used to power jet engines - can have a wide composition, mainly made up of paraffins and aromatics derived from oil. Like gasoline, each batch of jet fuel can have fluctuations in composition and is in principle different from any other. So, the specifications are not set on composition, but on fuel properties (e.g. Table 1.1).

1.3.1 Jet fuel standards

The main standards used worldwide are the ones from United States:

- JET A and JET A-1 are kerosene-based fuels (they differ by the maximum freezing point allowed) defined by the standard ASTM D1655 (9).
- JET B is a naphtha-kerosene based fuel: it is lighter and with a lower freezing point respect to Jet A. For this is used in arctic regions, where the cold weather conditions can cause problems of fuel freezing. In the rest of the world it's not common due to its higher flammability, source of safety concerns. It is defined by the standard ASTM D6615-15a (10).

- JP-1 to JP-8 are standards used in the military, being JP-4 the equivalent of civil Jet B and JP-8 the correspondent of Jet A-1

	JET A	JET A-1	JET B
Flash point (min)	38°C	38°C	-18°C
Freezing point (max)	-40 °C	-47 °C	-60 °C
Energy density	35.3 MJ/l	34.7 MJ/l	33.18 MJ/l
Density at 15°C	0.820 kg/l	0.804 kg/l	0.764 kg/l

Table 1.1: Jet fuel properties

Some other countries have defined their own standards ([11](#)): TS-1 and T-1 to T-8 are used in Russia, while RP-1 to RP-5 are used in China. However, the most common and the standard *de facto* is the JET A-1.

1.3.2 Jet fuels requirements

Here are reported the main properties that are usually specified for a jet fuel:

- **Energy content** ([12](#)). Since airplanes must minimize both their weight and their size for an efficient service, fuel tanks can't be too big (normally they are located on the bottom of the fuselage and inside the wings). The fuel should then have a high energy per unit of volume (energy density) and also a high energy per unit mass (specific energy).
- **Freezing point** and **viscosity** ([12](#), [13](#)). Since a jet fuel can be exposed to extremely low temperatures, especially at high altitudes, it is

necessary to ensure that the fuel remains a liquid also at those temperatures, that's why the freezing point is a crucial parameter. Moreover, the fluidity of a fuel is influenced by its viscosity. Since it is injected as a spray in the combustion chamber, in order to follow a certain spray design, viscosity should not be too high. On the other hand, viscosity should not be too low either, since the fuel itself acts as a lubricant in some moving parts of the engine, and lubricity depends on viscosity.

- **Flash point** ([12](#), [13](#)). Flash point is the minimum temperature at which the fuel's vapors are able to be ignited by an ignition source. This parameter is important for safety reasons.
- **Sooting tendency** ([14](#)). Particulate can be formed inside the engine during the combustion. It can lead to hotspot problems in the combustion chamber's walls due to the radiative heat transfer, that becomes relevant when the particulate is heated up to incandescence. Also, if not completely burned, soot particles can lead to erosion and clogging problems in some of the turbine components. In general, sooting tendency is a monotone function of the aromatic content - another parameter that can be specified.
- **Stability** ([12](#)).
Storage stability is the ability of the fuel to not undergo any relevant change as time passes, independently on the external environment (in typical conditions). This parameter has the highest importance in military, where fuels can be stored for long periods, in contrast to civil aviation, where fuels are used after a short time since their production.

Many chemical reactions can happen within the fuel: to reduce their impact, additives can be mixed with the fuel.

Thermal stability, on the other hand, shows its importance in the operations phase, during the voyage. Fuel is in fact often preheated before entering the combustion chamber: if any soot is formed during this phase, it can lead to the same problems described above.

- **Volatility** (12). The fuel's volatility should be high enough to let it vaporize when it is burnt, but not too high in order to avoid losses. This property is often reported by means of vapor pressure and distillation curve.

Some common additives for jet fuels are (15):

- **Antioxidants**. These additives may be used to prevent the formation of gum and other oxidation products.
- **Metal deactivators**. These additives can be included to improve the fuel's thermal stability by mitigating the effects of dissolved trace metals (e.g. Cu) which can compromise the thermal stability of jet fuels.
- **Corrosion inhibitors** allows to reduce oxidation and improve lubricating properties of the fuel, extending the fuel system operative life.
- **Fuel system icing inhibitors**. These compounds reduce the freezing point of any water that may be present in traces, preventing ice crystallization. Their use is mandatory in many military fuels, while they are

less common in civil aviation, where fuel heaters are more widespread.

- **Static dissipater additives** minimize the possibility of accumulation for static charges during fuel movements.

1.3.3 Approval of a new jet fuel

Since a jet fuel has to comply with a wide range of norms, it must behave as expected in many different situations and has a long list of safety standards to be assured, any candidate as a new jet fuel must undergo through numerous tests, both on ground and during flight, in many situations and conditions.

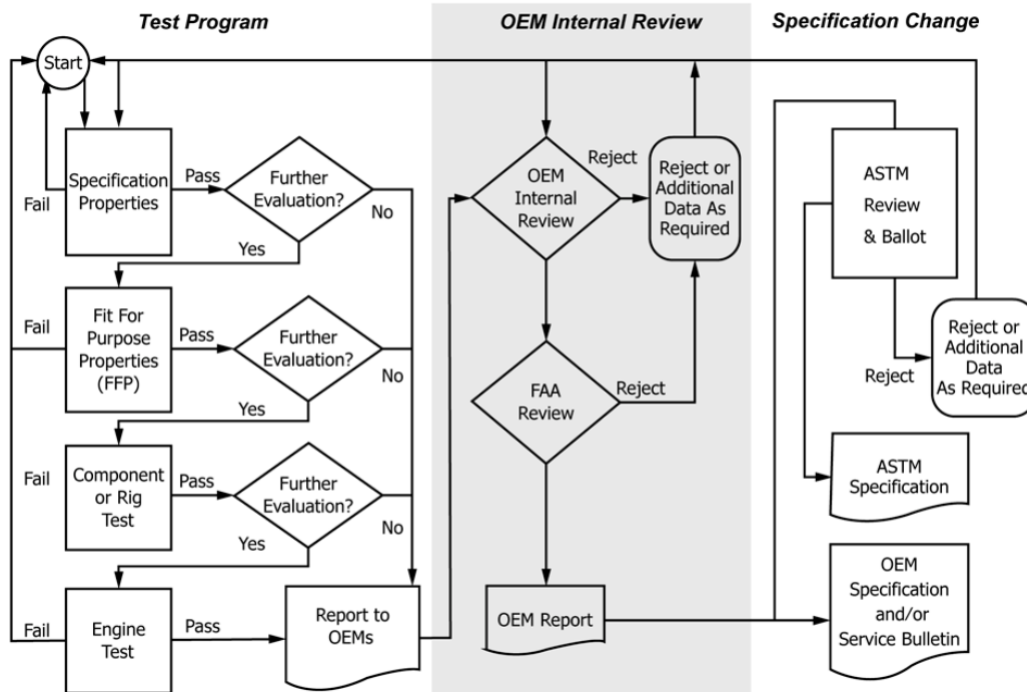


Figure 1.7: Overview Fuel and Additive Approval Process (16).

As example, the procedure for a new fuel approval in the USA is regulated by the ASTM D4054 ([16](#)) standard, and involves an extensive number of detailed tests (see Figure 1.7) to be carried out by the OEM (Original Equipment Manufacturer) of the jet engine, by the Federal Aviation Administration (FAA, the public aviation authority) and the ASTM (the institute of standards). This procedure may be particularly expensive and its duration can easily exceed some years. The combination of expenses and slowness is not compatible with a rapidly evolving energy scenario: an alternative route is necessary.

1.4 Aim of this work

It is obvious that the procedure just described cannot be applied for all fuel candidates, but a selection is required.

The aim of this work, a continuation of D. Demetryouss thesis work ([17](#)), is to develop models and procedures for the formulation of a jet fuel candidate by means of a **surrogate** fuel: i.e. a mixture that has the purpose to emulate one or more properties of the real fuel.

This mixture should have a composition much simpler than the real fuel, in order to be easily reproducible (preventing any effect of the real fuel's properties fluctuations). Moreover, a simple mixture is easier to be simulated on a computer, and the formulation of a virtual surrogate can save a lot of resources in selecting the candidates for real preliminary tests (that, later,

will lead to the bureaucratic procedure of approval described before).

Surrogates are often formulated by hand, relying heavily on the experience of the user. This work aims at automating the formulation procedure, shifting most of the work to the computer and requiring the user to provide only a palette of possible chemical compounds among which the program will select the best combination.

Obviously the code has many parameters that can be tuned, but the behavior of the code has been investigated, selecting a parameter set that can be considered satisfactory and is proposed by default.

After a brief introduction of the physical properties considered to evaluate the similarity between two mixtures and the numerical methods exploited through the whole work, reported in Chapter 2, an issue about mixing rules of ignition delay times and laminar burning velocities arose: their numerical evaluation would require excessive computational resources, so dedicated models needed to be derived to have a quick approximation of these properties. The development of the metamodel dedicated to ignition delay times is described in Chapter 3, while the construction of the metamodel for laminar burning velocities is the object of Chapter 4. Both these models are derived using the computational tools provided by the `OpenSMOKE++` suite ([18](#), [19](#)) and the kinetic mechanisms developed by the CRECK modeling group ([20](#)). Then the development of the formulation procedure is explained in Chapter 5: the transposition in a mathematical form of the problem of making many

properties as similar as possible (described as an optimization), the choice of an optimization routine, and the construction of an objective function are covered in this Chapter. The setting of parameters and the importance of each considered property is studied too. The framework is developed using Matlab[®].

In Chapter 6 the developed tool is tested and the surrogates for two real fuels are formulated. The obtained surrogates are compared with the ones proposed by others in the scientific literature, to check whether the code is valid.

At the end, in Chapter 7 the work is summarized, along with conclusions and possible future developments.

Chapter 2

Fuel properties and optimization algorithms

In this chapter the properties used to formulate the surrogate and their mixing rules are presented (i.e. the information required about the fuel of which a surrogate is requested and the information used to determine how similar the fuel and the surrogate are).

Then the algorithms exploited in the later chapters, together with a brief description of their working principles are discussed.

2.1 Chemico-physical properties

The formulation of a jet fuel surrogate is based on an optimization process that minimizes the difference in properties between the surrogate and the real fuel. The following properties are considered in this work:

- Molecular weight
- Hydrogen over carbon ratio
- Cetane number
- Density
- Viscosity
- Yield sooting index
- Distillation curve
- Ignition delay times curve
- Laminar burning velocity curve

The scalar properties are determined according to the following rules, being x_i the molar fractions of the surrogate (a complete description of symbols used is reported at page 116):

- MOLECULAR WEIGHT (MW)

Considering an atomic weight of 1 g/mol for hydrogen and 12 g/mol for carbon, the molecular weight is computed as:

$$MW_{surr} = 1 \sum_{i=1}^{N_{sp}} x_i n_{H_i} + 12 \sum_{i=1}^{N_{sp}} x_i n_{C_i} \quad (2.1)$$

- HYDROGEN / CARBON RATIO (H/C)

Similarly, the H/C ratio of the surrogate is computed as:

$$\frac{H}{C}|_{surr} = \frac{\sum_{i=1}^{N_{sp}} x_i \cdot n_{H_i}}{\sum_{i=1}^{N_{sp}} x_i \cdot n_{C_i}} \quad (2.2)$$

- DENSITY (ρ)

Density is computed as sum weighted by molar fractions (recall that

the fuel is liquid), as:

$$\rho_{surr} = \sum_{i=1}^{N_{sp}} x_i \cdot \rho_i \quad (2.3)$$

- YIELD SOOTING INDEX (YSI)

YSI value is computed weighting on mass fractions instead, as:

$$YSI_{surr} = \sum_{i=1}^{N_{sp}} \omega_i \cdot YSI_i \quad (2.4)$$

being the mass fractions ω_i linked to the molar ones through the relation

$$\omega_i = x_i \cdot \frac{MW_i}{MW_{surr}} \quad (2.5)$$

- CETANE NUMBER (CN)

The cetane number is computed as sum weighted on volume fractions:

$$CN_{surr} = \sum_{i=1}^{N_{sp}} V_i \cdot CN_i \quad (2.6)$$

where volume fractions V_i can be derived from mass fractions as

$$V_i = \frac{\omega_i / \rho_i}{\sum_{i=1}^{N_{sp}} \omega_i / \rho_i} \quad (2.7)$$

- VISCOSITY (μ)

Viscosity is expressed according to the mixing rule proposed by Kendall et al. (21):

$$\mu_{surr} = \left(\sum_{i=1}^{N_{sp}} \omega_i \cdot \mu_i^{1/3} \right)^3 \quad (2.8)$$

Note that each μ_i is function of temperature, here described as

$$\log_{10}(\mu_i(T)) = \alpha_i + \frac{\beta_i}{T} + \gamma_i \cdot T + \delta_i \cdot T^2 \quad (2.9)$$

where α_i , β_i , γ_i and δ_i are species-related constants.

In addition to these scalar quantities, several curves are considered too:

- **DISTILLATION CURVE**

The distillation curve is obtained solving the Rachford-Rice equation (22),

$$\sum_{i=1}^{N_{sp}} \frac{x_i \cdot (K_i - 1)}{1 + \alpha \cdot (K_i - 1)} = 0 \quad (2.10)$$

that describes the flash condition, as the mixture evaporates (this is obtained changing the vaporization ratio α).

The coefficients K_i , defined as

$$K_i \stackrel{def}{=} \frac{y_i}{x_i} = \frac{\text{molar fraction of } i \text{ in the vapor phase}}{\text{molar fraction of } i \text{ in the liquid phase}} \quad (2.11)$$

are computed expressing the vapor pressure according to Antoine equation and considering an ideal system:

$$K_i(T) = \frac{P_i^o(T)}{P} = \frac{10^{(A_i - B_i/(T + C_i))}}{P} \quad (2.12)$$

If at each step α is changed by δ , in that step the volume evaporated will be $\delta \cdot \sum_{i=1}^{N_{sp}} (x_i \cdot MW_i / \rho_i)$. The solution of Rachford-Rice equation is carried out using secants method, described in detail in Section 2.3.1.

- **IGNITION DELAY TIMES and LAMINAR BURNING VELOCITIES**

These two curves are expensive to be determined: for this reason their direct evaluation in an iterative optimization process would be un-

feasible. The development of appropriate metamodels is the object of Chapters 3 and 4.

The numerical values considered are reported in Table 2.1.

Species	Chemical formula	Density [kg/m^3]	Cetane number	YSI
i-cetane	$C_{16}H_{34}$	793	15.0	31.0
n-decane	$C_{10}H_{22}$	730	65.5	7.4
n-dodecane	$C_{12}H_{26}$	750	72.9	9.8
n-heptane	C_7H_{16}	680	56.0	3.0
1,2,4-tri methylbenzene	C_9H_{12}	876.1	8.9	260.6
o-xylene	C_8H_{10}	880	7.0	193.1

Species	Antoine coefficients			μ coefficients			
	A_i	B_i	C_i	α_i	β_i	γ_i	δ_i
i-cetane	6.99021	1358.75	231.405	-4.847	1.06E+03	0.0079	-7.36E-06
n-decane	7.21745	1693.93	216.459	-6.0716	1.02E+03	0.0122	-1.19E-05
n-dodecane	7.22883	1807.47	199.381	-7.0687	1.25E+03	0.0137	-1.22E-05
n-heptane	7.04605	1341.89	223.733	-5.7782	8.06E+02	0.0134	-1.48E-05
1,2,4-tri methylbenzene	7.29329	1763.35	230.248	-8.4686	1.36E+03	0.0173	-1.46E-05
o-xylene	7.14914	1566.59	222.596	-7.8805	1.25E+03	0.0161	-1.40E-05

Table 2.1: Numerical values of the considered properties

In particular, the vapor pressure is evaluated according to the Antoine law

$$\log_{10}(P_i^o) = A_i - \frac{B_i}{T + C_i}$$

with P_i^o in [mmHg] and T in [$^{\circ}C$], while the viscosity calculation is carried out according to Equation 2.9, with μ in [cP] and T in [K].

2.2 Optimization algorithms

2.2.1 Introduction to constrained optimization

In this work optimization algorithms are widely exploited, so they are here briefly described.

Let $f : \mathbb{R}^n \rightarrow \mathbb{R}$ be the objective function. It is asked to find $\bar{x} \in \mathbb{R}^n$ such that $f(\bar{x})$ is the minimum value, with the additional request that several constraints are satisfied – such constraints can be equations $g_j(\bar{x}) = 0$ or inequalities $h_j(\bar{x}) \geq 0$. This is mathematically schematized as:

$$\begin{cases} \min_{\bar{x}} f(\bar{x}) \\ s.t. \bar{g}(\bar{x}) = \bar{0} \\ \bar{h}(\bar{x}) \geq \bar{0} \end{cases} \quad (2.13)$$

Optimization algorithms often exploit the derivatives of the objective function to reach the goal faster, and can be classified according to the order of the function derivative used. If such gradients (and Hessians) are not available in analytical form, some algorithms can estimate them numerically.

However, in this work it is expected to deal with complex functions, strongly nonlinear, that may be even not continuous. To avoid misleading derivatives estimations, here are preferred *heuristic* algorithms, that do not exploit the objective function derivatives of any order, but rely only on the objective function itself.

Algorithms considered are:

- Genetic algorithm (23)
- Particle Swarm algorithm (24)
- Pattern Search algorithm (25)
- Matlab[®]'s `fmincon`

2.2.2 Genetic algorithm

The genetic algorithm is an optimization routine based on the work of Holland (23) and developed following the rules of biological evolution and natural selection. This algorithm starts from a (typically random) set of sample points inside the domain, on which the objective function is evaluated. Each point has a *genotype* (its \bar{x}) and a *fitness* (the objective function value).

Using the information on such points, a new “generation” of points is derived by the algorithm, according to these rules:

- “Elites”, the best points of the previous generation, pass unchanged to the next generation
- “Crossover children” are points created from two “parent points” by randomly choosing each component from one of the parents
- “Mutation children” are points created by insertion of random changes (mutations) in one single point from the previous generation

The algorithm stops when generations come to a *stall* (i.e. when the change between one generation and the other is below a specified tolerance), the

change in function value drops below a given threshold, or when a maximum time/number of generations is exceeded.

The genetic algorithm implementation provided in Matlab[®] (available under the name "ga") allows to constrain some variables as integers, as described in the work of Deep et al. (26): this feature will be used in this work to select which chemical species will be included in a surrogate.

2.2.3 Particle swarm algorithm

The particle swarm algorithm has been proposed by Kennedy and Eberhart (24) and tries to recreate the behavior of birds and insects inside a swarm.

The algorithm starts from a random set of sample points (or *particles*) each with a position and a velocity in the domain. At each iteration, each particle checks the objective function values on his neighbor particles and points towards that value (with the addition of a random noise). Moreover, each particle stores in memory the position with the best function value that it found, making this information available for the whole swarm.

In this way, if a particle finds a promising region, the swarm will move to that region and search efforts will be concentrated there.

It is used the Matlab[®] implementation of this algorithm with the function "particleswarm".

2.2.4 Pattern search algorithms

The pattern search family of algorithms (used as its Matlab[®] implementation "patternsearch", part of direct search method) starts from a first guess, creates a mesh of points around it and evaluates the objective function in each mesh point. If a new point with a lower function value is found, it is used as new mesh center and the mesh size is increased; else, the mesh size is reduced.

Several "Poll methods" (i.e. ways to build the mesh) are provided, each characterized by *a search algorithm* (generalized pattern search **GPS**/generating set search **GSS**/mesh adaptive search **MADS**) and *a pattern* ($2N$ or $N + 1$), a set of vectors on which the mesh is based: it consists of a basis for \mathbb{R}^N space (vectors with only one nonzero component equal to 1) plus the same vectors with changed sign for the $2N$ pattern, or plus the vector with all elements equal to -1 for the $N + 1$ pattern.

The mesh is created by shifting the guess point by all vectors in the pattern set, scaled by the mesh size (**GSS** and **MADS** have some other refinements).

In this work the combination **GPS** – $2N$ is used.

More details about **GPS** can be found in the article by Audet et al. ([25](#)).

2.2.5 fmincon

fmincon is one of the standard algorithms provided by Matlab[®]. It implements the interior point algorithm (presented by Byrd, Gilbert and Nocedal

(27)). It has been considered even if it exploits numerical gradients with the idea to have a comparison with `patternsearch`.

2.2.6 Summary of optimization algorithms

Summarizing, between the algorithms presented, `patternsearch` and `fmincon` require a first guess to find the solution, while `ga` and `particleswarm` do not.

In addition, `ga` has the possibility of including discrete variables.

Such features are exploited in later chapters.

2.3 Root-finding algorithms

Root-finding algorithms are used to solve equations (in mathematical form, it is asked to find x such that $f(x) = 0$).

In this work, it is chosen to use the secant method to solve the Rachford-Rice equation (Eqn 2.10) with respect to temperature, required for the derivation of the distillation curve. It is a single function in one variable.

2.3.1 Secant method

The secant method requires two guesses: it linearizes the function between these two points and uses the new-found point to replace the oldest one. The algorithm is reported below:

1. Evaluate function in both points $y_1 = f(x_1), y_2 = f(x_2)$
2. Evaluate the slope of linearized equation $m = (y_2 - y_1)/(x_2 - x_1)$

3. Replace x_1 with x_2
4. Replace y_1 with y_2
5. Replace x_2 with $x_2 - y_2/m$ (the zero of linearized equation)
6. Evaluate the function in this new point $y_2 = f(x_2)$
7. Repeat 2-6 until the change in x or in y is below certain thresholds
(in this work have been considered a tolerance equal to 10^{-4} for the variable and equal to 10^{-6} for the function).

This method has been chosen instead of Matlab[®]'s built-in solver `fsolve` (28) as it showed a faster convergence.

Chapter 3

Derivation of a metamodel for ignition delay times

Among the properties presented in Chapter 2, for ignition delay times and laminar burning velocities mixing rules are not available.

However, it is possible to obtain them by carrying out a numerical simulation with `OpenSMOKE++`. Nevertheless, such simulation requires time and CPU power: this makes a direct implementation of `OpenSMOKE++` simulations inside an iterative code unfeasible.

A metamodel for ignition delay times (IDT) is developed through this chapter: it should give an approximation of the IDT value in reasonable times and allow its insertion in an iterative procedure.

Ignition delay time is defined as the time passed between the injection of the fuel in the combustion chamber and the appearance of a flame. It can also

be defined as time passed between the injection of the fuel and the rise in pressure caused by the combustion, as it occurs very close to the appearance of the flame and their time difference is often negligible.

Here it is assumed that the fuel is already in vapor phase – the previous evaporation of the liquid fuel was not considered. Such IDT is expected to be function of the initial temperature of the mixture, its pressure, the equivalence ratio* and the fuel composition.

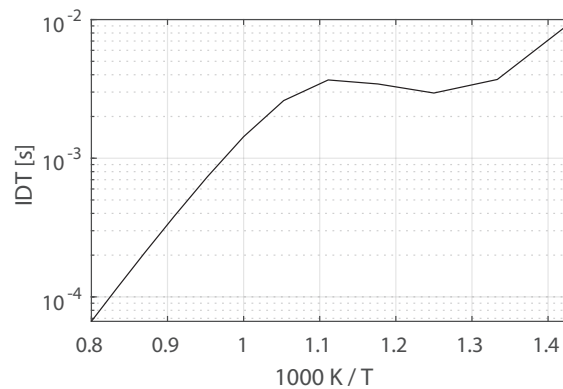


Figure 3.1: Example of IDT curve

IDTs are often reported as curves obtained changing temperature parametrically. A common chart displays IDTs on the vertical axis on logarithmic scale, plotted against the inverse of the temperature on the horizontal axis: an example is reported in Figure 3.1.

*The FUEL-AIR EQUIVALENCE RATIO, denoted by ϕ , is defined as the ratio between $n_{fuel}/n_{oxidizer}$ and the same quantity in stoichiometric conditions.

3.1 Species and operating conditions

To ensure reproducibility of the mixture, the number of chemical species used to formulate the surrogate should be kept as low as possible. However, the real fuels are characterized by a wide range of properties, that few components will never describe accurately.

Following the compromise presented by Narayanaswamy et al. (29), few species belonging to different chemical families are selected, in order to have "representatives" of the whole family's properties.

In this chapter the following species have been chosen (see also Figure 3.2):

- *isocetane* ($iC_{16}H_{34}$), for the family of branched alkanes
- *n-heptane* (nC_7H_{16}), *n-decane* ($nC_{10}H_{22}$) and *n-dodecane* ($nC_{12}H_{26}$) for the family of linear alkanes
- *1,2,4-trimethylbenzene* (tmbenz) and *o-xylene* for the family of aromatics

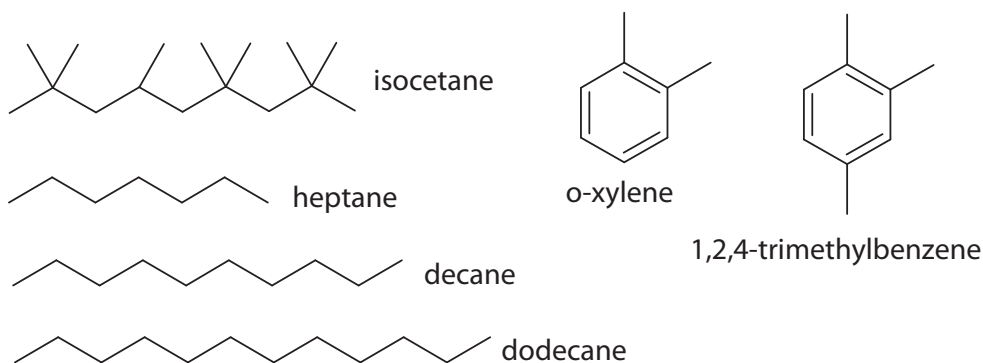


Figure 3.2: Considered species for the surrogate formulation

The metamodel should be able to approximate the IDT of any mixture of these 6 species. It has been chosen to describe the range of operative conditions reported in Table 3.1.

Variable	Lower limit	Upper limit
Temperature [K]	600	1200
Pressure [bar]	1	100
Equivalence ratio ϕ	0.5	2
Molar fractions x_i	0	1

Table 3.1: Ranges of conditions considered for IDT metamodel

3.2 Simulation of IDTs

3.2.1 The use of OpenSMOKE++ Suite

The detailed calculation of IDT is obtained by using the `OpenSMOKE++` Suite, and in particular the `OpenSMOKEpp.BatchReactor` solver. In fact, the suite includes a tool to estimate ignition delay times: it is solved an initial value problem (a system of ordinary differential equations + initial conditions,

reported here in Equation 3.1)

$$\left\{ \begin{array}{l} \frac{d}{dt}n_i = \dot{R}_i \cdot V \quad (\text{Mass balance for each species } i) \\ \frac{d}{dt}U = 0 \quad (\text{Energy balance}) \\ n_i|_{t=0} = n_i^0 \\ U|_{t=0} = U^0 \end{array} \right. \quad (3.1)$$

that represents a batch reactor. Looking at the trends obtained, the code can estimate when the combustion starts. Several rules are available (e.g. the time at which the slope of temperature or pressure profiles, or the amount of OH radicals exceeds a certain threshold is taken as IDT); in this work the combustion has been considered started when the time derivative of temperature exceeds a preestablished value.

The kinetic mechanism used is *POLIMI Primary Reference Fuels (PRF) + PAH + Real Fuels Low Temperature (LT)*, version 1412 (30), and the oxidizer considered is air (79% N_2 , 21% O_2).

Note that a low-temperature mechanism is chosen, as ignition involves reactions typical of this temperature range.

3.2.2 Outliers handling

This "virtual experiment" mode to estimate ignition delay times is not error-free, and sometimes the estimation of IDT values may fail.

A possible source of errors is the kinetic mechanism, that is a model itself

and will always be different from a real combustion.

Another source of errors can be the detection of the expected temperature trend, that in some cases may not be recognized (e.g. a temperature profile whose slope is under the numerical threshold considered won't be detected). For these reasons, before using these "raw" data, a procedure of outliers removal is carried out. In particular:

- any IDT value which is not included in the range between $3 \cdot 10^{-7}$ s and 1 s is removed (it is expected – and heuristically confirmed – that ignition delay times are in such orders of magnitude)
- IDT values that result different if computed according to different conditions (see section 3.2.1) are removed. The relative error threshold between these values is chosen as 15% (e.g. $1 - \tau_{P_{slope}}/\tau_{T_{slope}} < 0.15$). Moreover, if an IDT computed with any condition is exactly equal to 0 or 1, that IDT is removed.
- in addition, the IDT values that have passed the steps above are controlled by means of `rmoutliers` function provided by Matlab (31).

3.3 Data preprocessing

The problem can be schematized as follows: it is asked to find a metamodel $\hat{\tau}$ for the ignition delay times (IDT or τ) in function of temperature, pressure, equivalence ratio and fuel composition (having $N_{species}$ chemical compounds, τ is a function of $3 + N_{species}$ variables):

$$\tau = \tau(T, P, \phi, \bar{x}).$$

The reconstruction of a generic function in that many variables is complex.

To help the calculations, these measures have been adopted:

- The variable $\ln(\tau)$ is considered instead of the ignition delay time itself. Since it is expected that IDTs range on a wide band of orders of magnitude, the adoption of the natural logarithm allows to consider more similar numbers.
- Analogously, the variable $1000/T$, with T being the temperature in Kelvin, is considered in place of the temperature itself.
- The dependence on pressure is expected to be weaker than other variables. For this reason, a series of *reduced models* has been developed at fixed pressures $\tau = \tau(T, \phi, \bar{x})$. The pressure trend is assumed linear between the nearest reduced models. The pressure values considered are 1, 2, 3, 5, 10, 20, 30, 50, 70 and 100 bar.

3.4 Kriging models

However, the modelling of such reduced models remains complex, mainly due to the high number of variables (let $k = 2 + N_{species}$ be that number). To deal with this, it has been chosen to employ Kriging models, as described in the book by Forrester, Sóbester and Keane (32).

A complete description is available on the book, however, the idea on which these models are based is:

- The function to be modelled is expensive to be evaluated, so function evaluations should be kept as low as possible

- The function should be evaluated in points uniformly distributed in the k -dimensional space. Moreover, they should not be aligned in any direction – told in another way, if such points are projected on any of the variables' axis, they should be again uniformly distributed (see figure 3.3). The placement of sample points in the high-dimensional space is carried out using the `bestlh` function provided by the book (33), based on the Best Latin Hypercube method.

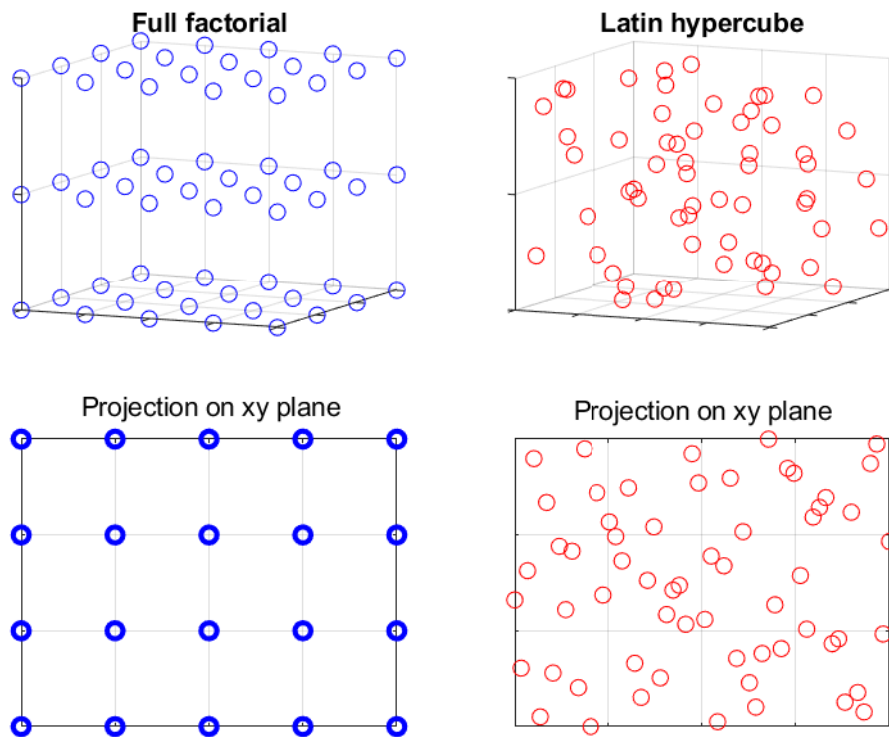


Figure 3.3: Comparison of full-factorial (structured) and latin hypercube methods to choose sampling points in a 3D space

- From Radial basis functions techniques comes the idea of superimposing many basis functions ψ , each centered on a sample point. These

functions are chosen of Gaussian type (exponents smaller than 2 could have been considered, but Gaussian functions have been preferred to avoid dealing with non-smooth functions)

Having NP sampling points, each of coordinate $\bar{c}_i \in \mathbb{R}^k$, the function to be modelled is built as:

$$f(\bar{x}) = \sum_{i=1}^{NP} (w_i \cdot \psi(\bar{x}, \bar{c}_i)) \quad (3.2)$$

where w_i are the weights associated to each basis function ψ .

From the choice of Gaussian functions it is derived the expression:

$$f(\bar{x}) = \sum_{i=1}^{NP} \left(w_i \cdot \exp \left(- \sum_{j=1}^k \vartheta_j \cdot |x_j - c_{i,j}|^2 \right) \right) \quad (3.3)$$

where the subscript j refers to the j -th dimension.

The parameters of this model, once the function is evaluated in the sample points \bar{c}_i , are then w_i (one for each sample point) and ϑ_j (one for each variable).

Of particular interest are the parameters ϑ_j , as they can be linked with a physical meaning: they measure how much the function to be modelled depends on that variable. On the other hand, the weights w_i can be computed automatically, as shown in (32). Being Ψ the matrix of the Gaussian basis functions evaluated for all couples of sample points and \bar{y} the vector of function evaluations, it must hold $\Psi \bar{w} = \bar{y}$. In addition, since Ψ results to be symmetric positive definite, it can be triangularized by means of Cholesky factorization ($\Psi = \mathbf{U}^\top \mathbf{U}$, with \mathbf{U} upper triangular). The weights can be

determined by solving the linear system $\mathbf{U}^\top \mathbf{U} \bar{w} = \bar{y}$.

However, Kriging models have been developed for interpolations. For our purposes of models construction, interpolation is not the best choice. Nevertheless, Kriging models can be extended to regressions by adding a scalar parameter λ to the main diagonal of Ψ , called regularization parameter. As this parameter tends to zero, the model tends to an interpolation of fit data.

3.4.1 Estimation of parameters

The estimation of parameters is carried out by maximization of the likelihood, defined as:

$$\ln(L) = -\frac{NP}{2} \ln(\hat{\sigma}^2) - \frac{1}{2} \ln(\det(\Psi)) \quad (3.4)$$

$$\text{with } \hat{\sigma}^2 = \frac{(\bar{y} - \bar{\mathbf{1}}\mu)^\top \Psi^{-1} (\bar{y} - \bar{\mathbf{1}}\mu)}{NP}, \text{ and } \mu = \frac{\bar{\mathbf{1}}^\top \Psi \bar{y}}{\bar{\mathbf{1}}^\top \Psi \bar{\mathbf{1}}}.$$

This optimization (the maximization of L is equivalent to the minimization of $-\ln(L)$) is carried out using the `particleswarm` algorithm (also `ga` has been considered, but `particleswarm` has been chosen for its faster convergence, an important aspect given that many reduced models must be built). The unknown parameters ϑ_j, λ are researched in 10-base logarithmic scale, with bounds for low-pressure reduced models reported in table 3.2.

For higher-pressure models, since it is expected that ϑ_j parameters don't change too much with pressure, the search bounds are reduced to the parameters estimated at lower pressure plus or minus a small variation, in the order of 10^{-1} on logarithmic scale.

	min	max
ϑ	10^{-3}	10^2
λ	10^{-6}	10^0

Table 3.2: Upper and lower limits for parameters ϑ and λ

It was noticed that this helps the optimization routine, which else would be required to search in a much wider region of the k-dimensional space.

3.4.2 Addition of points

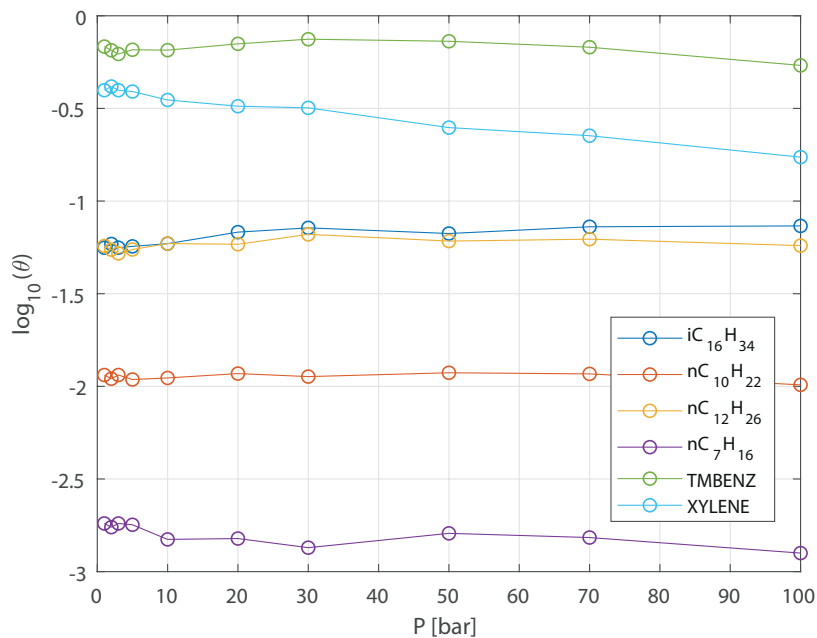
An interesting characteristic of Kriging models is that they allow one to find new sample points, where an additional function estimation (in this case, an IDT simulation) would provide more benefits to the model. This new point is found by means of the function `reintpredictor` provided by (33).

In this work such function has been implemented in a way that, if a point is detected as outlier and must be removed, it is replaced by a new point determined with this method. This ensures that the metamodel will be based on the exact number of points specified by the user.

Here the chosen number of sample points is equal to 100.

3.5 Results

The obtained results are reported in detail in Appendix A, while the estimated ϑ parameters for each species are reported in Figure 3.4.

Figure 3.4: Trends of ϑ parameters with respect to pressure

From the physical meaning of ϑ it's possible to see that xylene and trimethylbenzene – the aromatic species considered - have the largest impact on ignition delay times.

On the other hand, it seems that n-heptane has a very low influence on ignition delay times, but this can be explained by the presence of n-decane and n-dodecane: these three linear alkanes have similar properties, and the contribution given by n-heptane can be described also from n-decane and n-dodecane. Since other models with a lower number of species have been considered, this has been taken as a signal that 6 chemical compounds are enough to describe ignition delay times, and the model built with 6 species has been used as metamodel to be used for later surrogate optimization.

3.6 Model verification

The developed model has been tested with two methods:

1. one is the comparison of the model output with the detailed calculations for several points. this should verify whether the model fits well not only in the points used for its construction.
2. the other is the simulation of several IDT curves and, combining the model and an optimizer, to reconstruct the mixture composition that produces that curve. This should check whether it is possible to use the model to fit a known curve.

First test method

Regarding the first method, about 47000 points (47338) have been simulated for validation, giving an R^2 value of 0.9985[†].

To have a graphical representation of this, some sets composed by 500 points have been extracted and their parity plots are reported in Figure 3.5: in an ideal situation the points in these plots should stay on the main diagonal.

[†]The R^2 value, or *coefficient of determination*, can be used to estimate how good the data set produced by the model \hat{y}_i fits the real (in this case, simulated) data set y_i . It is defined as $R^2 = 1 - SS_{res}/SS_{tot}$, with $SS_{res} = \sum_i (y_i - \hat{y}_i)^2$ and $SS_{tot} = \sum_i (y_i - \text{mean}(y_i))^2$

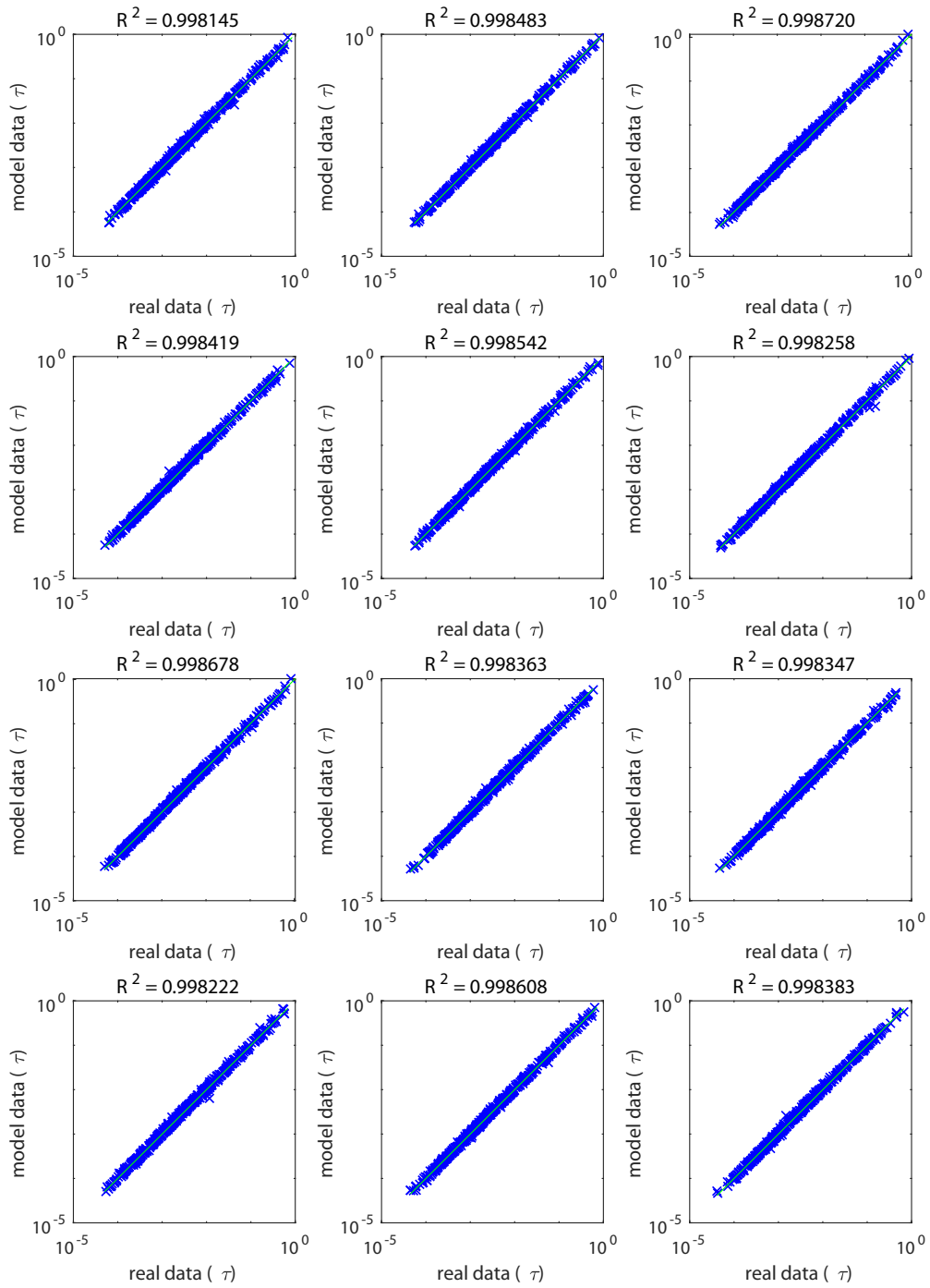


Figure 3.5: Validation of 12 sets of 500 points with the 6 component Kriging model

These data are used also to test where the model fits better and where it is worse: as reported in Table 3.3, it's seen that the model fits a little better at lower temperatures and at higher pressures (in any case without a significant loss of performance, so that the model is considered valid for the whole range of conditions considered).

Variable	Range	R^2	# of points
T	600-800 K	0.9977575	16025
T	800-1000 K	0.9971732	15974
T	1000-1200 K	0.9968744	15339
P	1-2 bar	0.9958473	1306
P	2-5 bar	0.9970973	4132
P	5-10 bar	0.9962480	6776
P	10-20 bar	0.9957476	13423
P	20-50 bar	0.9978576	12426
P	50-100 bar	0.9975807	9275
ϕ	0.5-1.0	0.9981445	15577
ϕ	1.0-1.5	0.9988567	15727
ϕ	1.5-2.0	0.9983856	16034

Table 3.3: Values of R^2 computed on subsets of validation simulations, each obtained by bounding one variable

Second test method

About the second method, few mixtures with known compositions are selected. Once chosen to fix pressure at 15 bar and to simulate temperatures spaced by 50 °C, it is reconstructed the target IDT curve using `OpenSMOKE++`. Having this data, it is asked to an optimizer (in this case, `ga`) to find the fuel composition in order to minimize

$$f_{obj}(\bar{x}) = \sum_{i=1}^{N_{points}} \left(1 - \frac{\tau_{i,model}}{\tau_{i,target}} \right)^2 \quad (3.5)$$

In this case three tests have been carried out. The mixtures considered are here reported in Table 3.4.

Composition [%]	Target mixtures			Found (optimized) mixtures		
	Mix#1	Mix#2	Mix#3	Mix#1	Mix#2	Mix#3
iC ₁₆ H ₃₄	75	60	40	60.67	71.65	44.67
nC ₁₀ H ₂₂	-	-	25	28.37	-	-
nC ₁₂ H ₂₆	-	-	-	-	-	25.70
nC ₇ H ₁₆	15	-	-	-	-	9.41
tmbenz.	-	40	-	10.96	28.35	-
o-xylene	10	-	35	-	-	20.22

Table 3.4: Compositions of some test mixtures and their optimized surrogates

It's possible to see that mixtures are not found with great accuracy, however this result is accepted, as at least the chemical families are somehow recognized and the only objective function, the difference of IDT curves, is

effectively minimized, as shown in Figure 3.6.

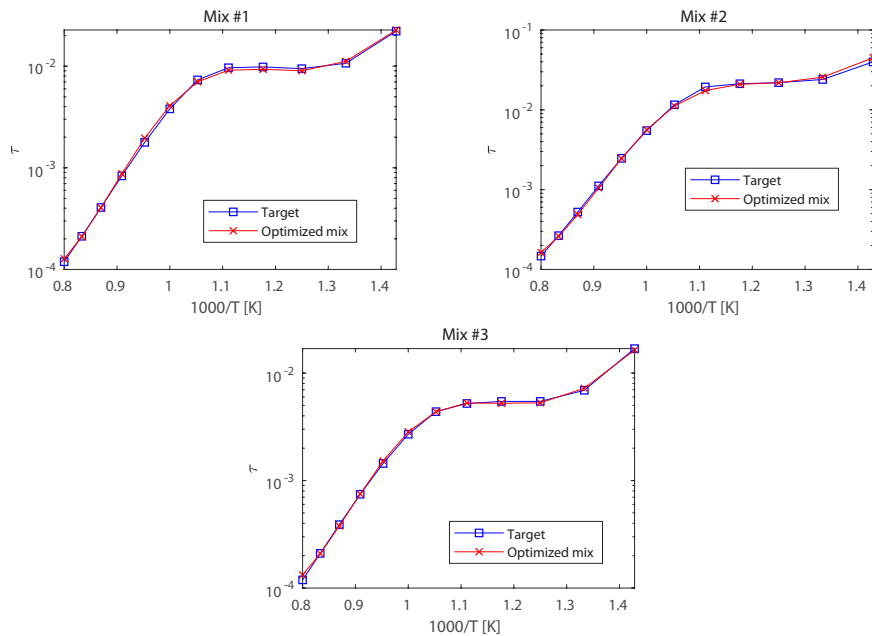


Figure 3.6: IDT curves for target and optimized mixtures

3.7 Summary

In this chapter the problem of describing the ignition delay times of mixtures has been faced.

Using the Kriging approach, a metamodel was developed, exploiting numerical OpenSMOKE++ simulations to build it. The model has also been verified: it is now possible to use it as a replacement for slower detailed simulations in the context of the surrogates formulation.

In the next chapter a similar problem for laminar burning velocities is faced.

Chapter 4

Derivation of a metamodel for laminar burning velocities

In this chapter the derivation of a mixing rule for laminar burning velocities is described.

As for ignition delay times, the use of the `OpenSMOKE++` Suite allows to evaluate laminar burning velocities, but with the drawback of the high computational cost that prevents the direct implementation in an iterative code. In this case the CPU time required by a simulation is increased by more than 2 orders of magnitude respect to the previous chapter.

Laminar burning velocity, or LBV, represents the speed with which the flame front moves in an unburnt gas. Such property will be a function of the mixture composition, of its temperature and pressure. A common way to characterize a fuel is to construct a curve that describes how the laminar burning

velocity changes with the equivalence ratio, at fixed initial temperature and pressure. An example is reported in Figure 4.1

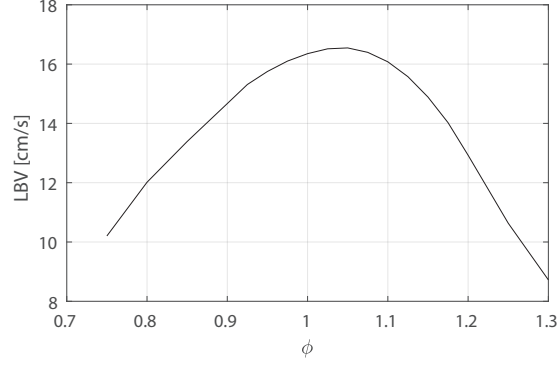


Figure 4.1: Example of LBV curve

4.1 Simulation of LBV

LBVs can be measured in the situation of a flame in laminar regime as the propagation velocity of the flame front.

Such situation can be mathematically schematized as a one-dimensional boundary value problem (BVP - reported in Equations 4.1) between the condition of unburnt gas and burnt gas.

$$\left\{ \begin{array}{l} \frac{d(\rho v)}{dx} = 0 \\ \rho v \frac{d\omega_i}{dx} = -\frac{dj_i}{dx} + \dot{m}_i \\ \rho v c_p \frac{dT}{dx} = \frac{d}{dx} \left(\lambda \frac{dT}{dx} \right) - \sum_{i=1}^{N_{sp}} \left(h_i \dot{m}_i + c_p j_i \frac{dT}{dx} \right) \\ + \text{Boundary conditions} \end{array} \right. \quad (4.1)$$

In this work detailed simulations of LBVs are run using the `OpenSMOKE++` suite by means of the solver `OpenSMOKEpp_PremixedLaminarFlame1D`, that implements the solution of the problem described in Equations 4.1.

Due to the long times required by the simulation (on the calculator used in this work*, the computation of a single LBV curve required about 16 hours), it is necessary to find a quicker way to evaluate LBVs: a metamodel is then required.

4.2 Polynomial models

However, for the same reason, such metamodel should be developed with a minimal data set, in order to build the model in reasonable times.

What here is proposed is to use as starting point the LBV curves of the pure compounds at the desired initial temperature and pressure (demanding to the user the input of these data) and to develop a mixing rule as function of the compositions only. Carrying on the work of D. Demetryouss ([17](#)), polynomial models are investigated: thanks to their relative simplicity they can be built with few known data. Moreover, LBVs did not show any particular nonlinearity, differently from IDTs.

From the work by Sileghem et al. ([34](#)), it's expected that each component of the mixture will have a weight proportional to its molar fractions: following this idea to express the polynomial coefficients, it's obtained an expression

*3.07 GHz Intel® Xeon® X5675 CPU and 32 GB of RAM

like

$$\begin{aligned}
s_L^{mix} = & \sum_{i=1}^{N_{Species}} \alpha_i x_i s_{L,i} + \sum_{i=1}^{N_{Species}} \sum_{j=1}^i \beta_{ij} (x_i s_{L,i}) (x_j s_{L,j}) + \dots \\
& + \sum_{i=1}^{N_{Species}} \sum_{j=1}^i \sum_{k=1}^j \gamma_{ijk} (x_i s_{L,i}) (x_j s_{L,j}) (x_k s_{L,k}) \dots \quad (4.2)
\end{aligned}$$

In this work the following possibilities have been explored:

- Model #1 - A 1st order polynomial (i.e. a linear combination)

$$s_L^{mix} = \sum_{i=1}^{N_{Species}} \alpha_i x_i s_{L,i} \quad (4.3)$$

- Model #2 - A 2nd order polynomial, considering only the terms referred to a single species

$$s_L^{mix} = \sum_{i=1}^{N_{Species}} (\alpha_i x_i s_{L,i} + \beta_i (x_i s_{L,i})^2) \quad (4.4)$$

- Model #3 - A 3rd order polynomial, considering only the terms referred to a single species

$$s_L^{mix} = \sum_{i=1}^{N_{Species}} (\alpha_i x_i s_{L,i} + \beta_i (x_i s_{L,i})^2 + \gamma_i (x_i s_{L,i})^3) \quad (4.5)$$

- Model #4 - A 2nd order polynomial, considering both the terms referred to single species and to many of them

$$s_L^{mix} = \sum_{i=1}^{N_{Species}} \alpha_i x_i s_{L,i} + \sum_{i=1}^{N_{Species}} \sum_{j=1}^i \beta_{ij} (x_i s_{L,i}) (x_j s_{L,j}) \quad (4.6)$$

The developed framework allowed to build also higher order models, but these models have been considered satisfactory. Moreover, models considering polynomials of order higher than 3 showed the first evidences of overfitting.

4.3 Parameter estimation

In order to estimate parameters, LBV curves in conditions reported in Table 4.1 have been simulated.

Inlet temperature	298 K
Pressure	15 atm
Kinetic mechanism	POLIMI_PRF_PAH_RFUELS_HT_1412 <i>POLIMI Primary Reference Fuels (PRF) + PAH + Real Fuels HT (Version 1412)</i>
Oxidizer	Air (79% N ₂ + 21% O ₂ in moles)
ϕ values	0.75 0.80 0.85 0.90 0.925 0.95 0.975 1.0 1.025 1.05 1.075 1.10 1.125 1.15 1.175 1.20 1.25 1.30 1.35 1.40 1.45 1.50

Table 4.1: Simulation conditions for laminar burning velocities

The curves used to fit the parameters are obtained from these mixtures:

- all the pure compounds (reported in Figure 4.2)
- all the equimolar binary mixtures (i.e. mixtures composed by two species with a ratio 1:1)

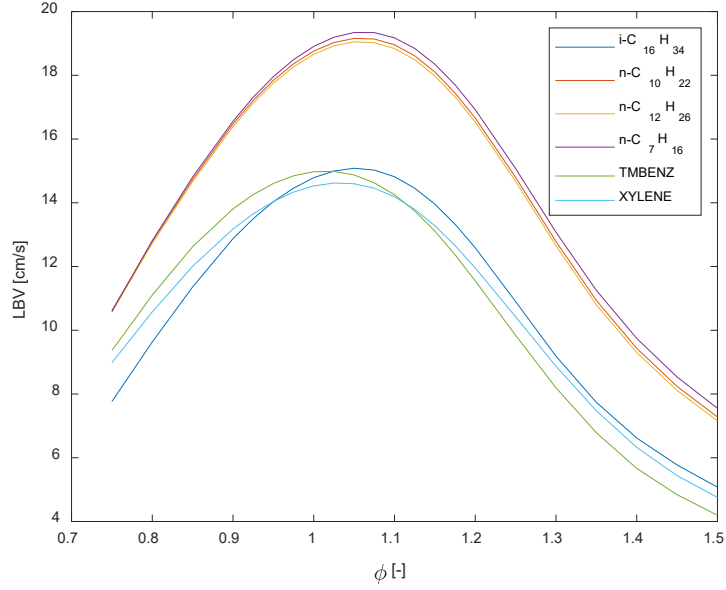


Figure 4.2: LBV curves for pure components

- all the equimolar ternary mixtures (i.e. mixtures composed by three species with a ratio 1:1:1)

The estimation of parameters is schematized as the minimization of

$$\min_{\alpha, \beta, \gamma} \sum_{i=1}^{N_{Points}} \frac{(\hat{s}_{L,i} - s_{L,i})^2}{s_{L,i}^2} \quad (4.7)$$

where \hat{s}_L is the laminar burning velocity predicted by the model, while s_L is the one simulated with `OpenSMOKE++`.

The optimization routine used in this case is `ga` (genetic algorithm). After some trials-and-errors, the optimization boundaries reported in Table 4.2 have been chosen.

Parameters	Min. Value	Max. Value
α (1 st order)	0.5	1.1
β (2 nd order)	-0.005	0.02
γ (3 rd order)	-0.001	0.001

Table 4.2: Boundaries for LBV model parameters

An exception has been done for model #4: its parameters have been estimated by means of `patternsearch` and using as first guesses for α and β the ones obtained for the model #2. This has been done due to the high number of parameters (model #4 has 27 parameters, respect to the 6, 12 and 18 parameters of models #1, #2 and #3). The use of a first guess helped the optimizer in solving the 27-dimensional problem.

4.4 Obtained parameters

The found parameters for models #1, #2 and #3 are reported in Table 4.3 and on Figure 4.3, while parameters for model #4 are reported in Table 4.4.

Model	#1	#2		#3		
Parameter	α_i	α_i	β_i	α_i	β_i	γ_i
iC ₁₆ H ₃₄	0.9517	0.8786	9.81E-03	0.8539	1.81E-02	-5.26E-04
nC ₁₀ H ₂₂	0.9980	0.9887	1.43E-03	0.9565	9.75E-03	-4.08E-04
nC ₁₂ H ₂₆	1.0106	1.0162	-1.69E-04	1.0006	4.53E-03	-2.56E-04
nC ₇ H ₁₆	0.9729	0.9326	4.76E-03	0.8941	1.45E-02	-4.65E-04
tmbenz	1.0239	1.0520	-2.97E-03	0.9929	1.49E-02	-1.05E-03
o-xylene	1.0146	1.0259	-8.70E-04	0.9588	2.00E-02	-1.25E-03

Table 4.3: Obtained parameters for LBV model #1 - #3

It is possible to see that the first order parameters (α_i) are all close to 1, while higher order parameters have a low value: this allows to state that a simple linear mixing rule weighted on molar fraction is adequate, at least as a first approximation.

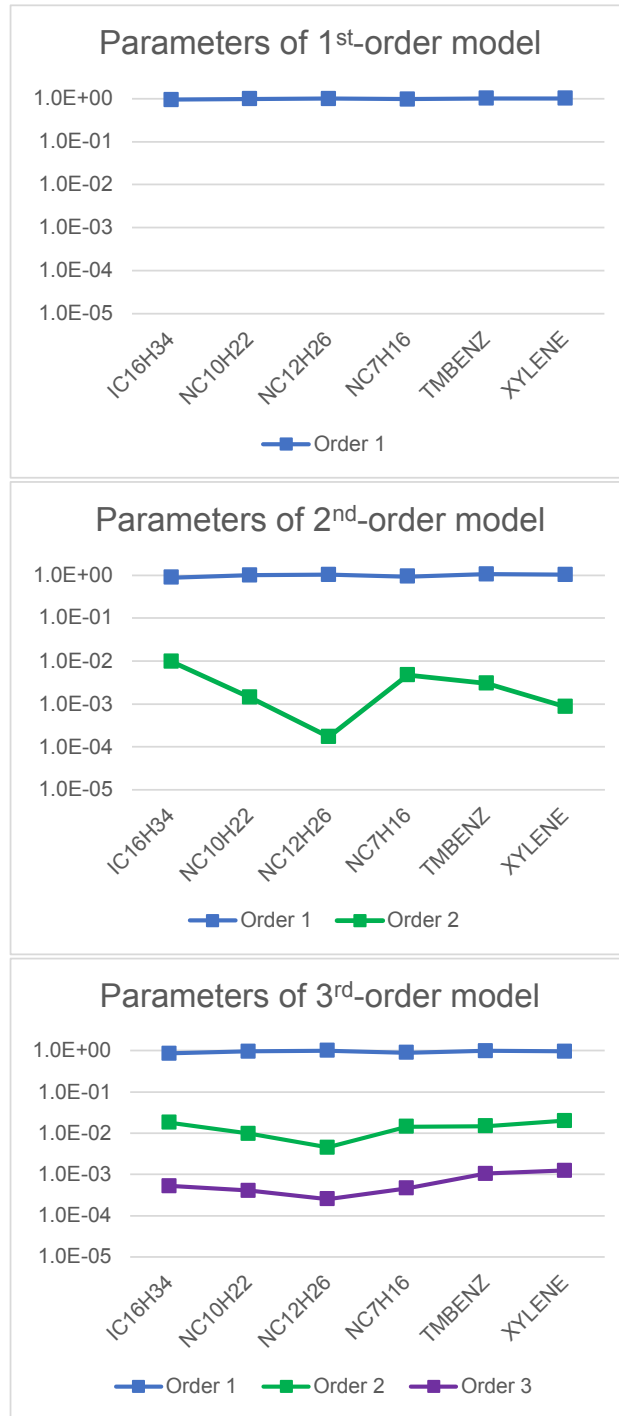


Figure 4.3: Obtained parameters for LBV models #1 - #3, in absolute value

Parameter	α_i	β_{ii}		β_{ij}		β_{ij}
iC ₁₆ H ₃₄	0.8849	0.00944	iC ₁₆ H ₃₄ -nC ₁₀ H ₂₂	-0.00131	nC ₁₀ H ₂₂ -XYLENE	0.01172
nC ₁₀ H ₂₂	0.9595	0.00242	iC ₁₆ H ₃₄ -nC ₁₂ H ₂₆	-0.00040	nC ₁₂ H ₂₆ -nC ₇ H ₁₆	0.00699
nC ₁₂ H ₂₆	0.9891	0.00066	iC ₁₆ H ₃₄ -nC ₇ H ₁₆	-0.00278	nC ₁₂ H ₂₆ -TMBENZ	0.01126
nC ₇ H ₁₆	0.9005	0.00596	iC ₁₆ H ₃₄ -TMBENZ	0.00955	nC ₁₂ H ₂₆ -XYLENE	0.01248
TMBENZ	1.0021	-0.00014	iC ₁₆ H ₃₄ -XYLENE	0.01117	nC ₇ H ₁₆ -TMBENZ	0.00980
XYLENE	0.9633	0.00305	nC ₁₀ H ₂₂ -nC ₁₂ H ₂₆	0.00345	nC ₇ H ₁₆ -XYLENE	0.01074
			nC ₁₀ H ₂₂ -nC ₇ H ₁₆	0.00891	TMBENZ-XYLENE	0.00293
			nC ₁₀ H ₂₂ -TMBENZ	0.01068		

Table 4.4: Obtained parameters for LBV model #4

Having these parameters, the metamodel is now available for the surrogate formulation procedure, requiring as input the LBV curves of the pure compounds.

4.5 Model verification

The developed model is now verified, using the same methods used for ignition delay times, as reported in Section 3.6.

First test method

All the models derived have been verified using 24 mixtures with random composition: the forecasts of the polynomial model are compared with detailed OpenSMOKE++ simulations.

The test with the 12th random mixture are reported in Figure 4.4 as example.

The mixture has a molar composition:

iC ₁₆ H ₃₄ :	0.2924
nC ₁₀ H ₂₂ :	0.0874
nC ₁₂ H ₂₆ :	0.3337
nC ₇ H ₁₆ :	0.1257
TMBENZ:	0.0705
XYLENE:	0.0901

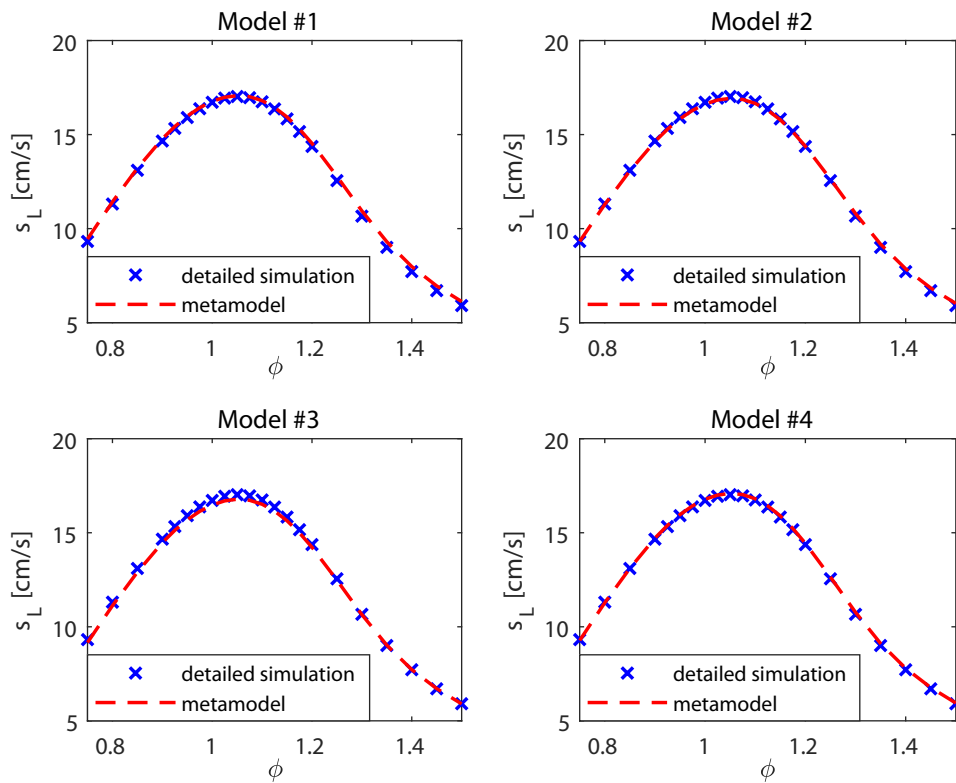


Figure 4.4: Validation of LBV models with a random mixture

The average R^2 value on these 24 validation sets are here reported in Table 4.5.

	Model #1	Model #2	Model #3	Model #4
R^2	0.99815	0.99767	0.99642	0.99947
# of parameters	6	12	18	27

Table 4.5: R^2 values for the validation mixtures

This shows that the inclusion of terms referred to more species allows the polynomial model to perform better. However, all models are considered satisfactory.

Second test method

A further test method is considered: some mixtures are chosen, and their LBV curves are built via `OpenSMOKE++` simulations.

Once the curves are known, it is asked to an optimizer (again, `ga`) to find the fuel composition in order to minimize:

$$f_{obj}(\bar{x}) = \sum_{i=1}^{N_{points}} \left(1 - \frac{s_{Li,model}}{s_{Li,target}} \right)^2 \quad (4.8)$$

Also in this case, as for ignition delay times, three tests have been carried out. The mixtures considered are here reported in Table 4.6 and their LBV curves in Figure 4.5.

As for the IDT case, it can be noted that the polynomial model was able to reproduce with a good accuracy the target curves, showing the appropriate-

	Original / Target	Mixtures found using			
		Model #1	Model #2	Model #3	Model #4
1	iC ₁₆ H ₃₄ 0.6	iC ₁₆ H ₃₄ 0.6498	iC ₁₆ H ₃₄ 0.6057	iC ₁₆ H ₃₄ 0.5936	iC ₁₆ H ₃₄ 0.5796
	o-xylene 0.4	nC ₁₂ H ₂₆ 0.0722	nC ₁₀ H ₂₂ 0.0726	nC ₇ H ₁₆ 0.088	nC ₇ H ₁₆ 0.0629
		o-xylene 0.2779	o-xylene 0.3216	o-xylene 0.3184	o-xylene 0.3574
2	iC ₁₆ H ₃₄ 0.45	iC ₁₆ H ₃₄ 0.4956	iC ₁₆ H ₃₄ 0.4303	iC ₁₆ H ₃₄ 0.4461	iC ₁₆ H ₃₄ 0.4411
	nC ₁₀ H ₂₂ 0.25	nC ₁₂ H ₂₆ 0.2457	nC ₇ H ₁₆ 0.2954	nC ₁₂ H ₂₆ 0.1426	nC ₇ H ₁₆ 0.3133
	tmbenz 0.3	tmbenz 0.2586	tmbenz 0.2742	nC ₇ H ₁₆ 0.1698	tmbenz 0.2456
			tmbenz 0.2415		
3	iC ₁₆ H ₃₄ 0.25	iC ₁₆ H ₃₄ 0.3761	iC ₁₆ H ₃₄ 0.3667	iC ₁₆ H ₃₄ 0.3561	iC ₁₆ H ₃₄ 0.2950
	nC ₁₀ H ₂₂ 0.20	nC ₁₂ H ₂₆ 0.2056	nC ₁₀ H ₂₂ 0.2292	nC ₁₂ H ₂₆ 0.1637	nC ₇ H ₁₆ 0.2320
	tmbenz 0.35	tmbenz 0.4184	tmbenz 0.4041	nC ₇ H ₁₆ 0.0911	tmbenz 0.3427
			tmbenz 0.3891	o-xylene 0.1302	

Table 4.6: Comparison of three 'target' mixtures and the mixtures obtained with models so that the LBV curve is well fitted

ness of the model to describe the mixing rule for LBVs.

However, the mixtures found matching the LBV curves can differ from the original one: this can be explained by the fact that some species may have a similar behavior, and the optimizer has more possibilities to build the mixture. This can be taken as a positive behavior, as the LBV curve will not excessively constrain the search for a surrogate.

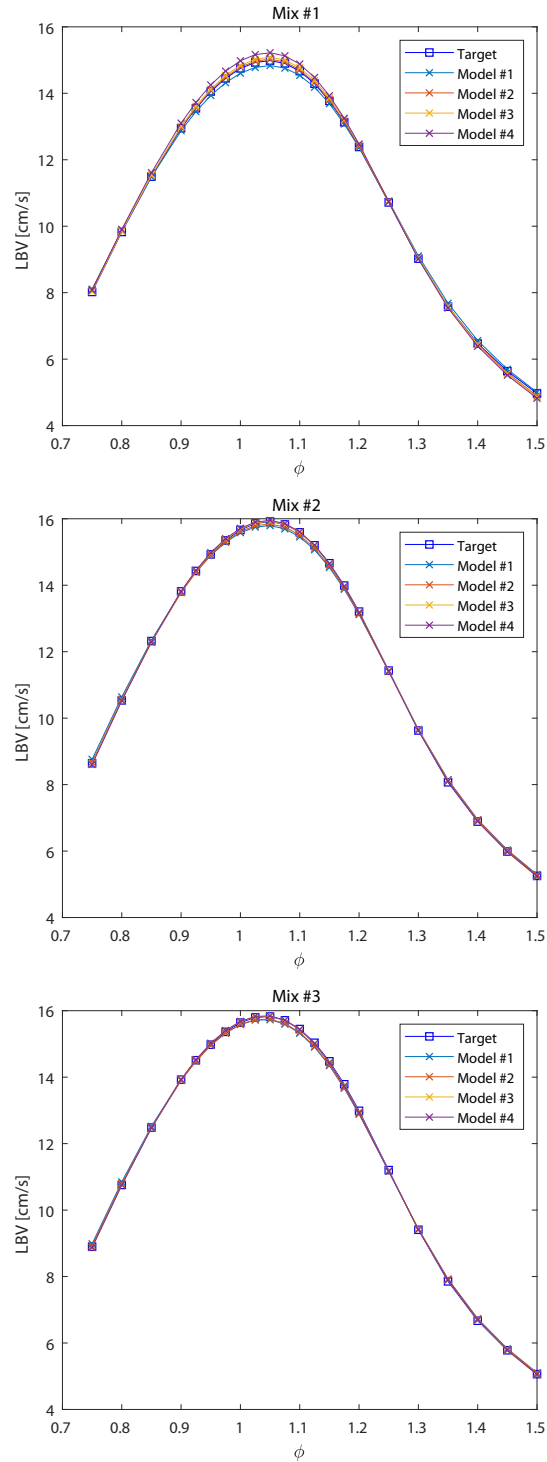


Figure 4.5: LBV curves for target and optimized mixtures

4.6 Summary

In this chapter an approximate mixing rule for the estimation of laminar burning velocities has been developed.

Due to the important computational resources required for the detailed LBV estimation, a polynomial combination has been selected, as it can be built using few known data. It was found that even a linear mixing rule weighted on molar fractions can describe with acceptable accuracy.

The model predictions have been verified: it is possible to use the derived model as a replacement for detailed simulations in the context of the surrogates formulation.

At this point all the required mixing rules are available: in the next chapter such mixing rules are used to develop the procedure for surrogates formulation.

Chapter 5

Development of an optimization strategy for surrogates formulation

Being available the models described in Chapters 2 - 4, it is now time to develop an optimization procedure for the surrogate formulation. The problem can be split in two main parts: the choice of the optimizer and the choice of the objective function. This chapter starts with the definition of the objective function shape, followed by a comparison of optimization routines, and ends with a review of which properties are required as input data for the procedure.

5.1 The objective function

The basic idea is to build the objective function as "difference" between the target fuel and the surrogate fuel, so that its minimization implies that the fuels' properties are as similar as possible.

For each property, say p , it's chosen to use the relative error -squared- between the surrogate fuel and the target fuel

$$\varepsilon_p = \left(1 - \frac{p_{surr}}{p_{target}}\right)^2$$

in order to have errors with the same order of magnitude.

In addition, to make curves comparable with scalar properties, when a curve is considered it is chosen to consider the average error for all the points of which the curve is made up. Say that the curve is built with N_p points, its error is computed as

$$\varepsilon_p = \frac{1}{N_p} \sum_{i=1}^{N_p} \left(1 - \frac{p_{i,surr}}{p_{i,target}}\right)^2$$

From chapter 3.3 recall the choice to consider the ignition delay times on a logarithmic scale.

Now, being available the errors' expressions, the objective function is built

as weighted linear combination of the errors related to all the properties:

$$\begin{aligned}
f_{obj} = & w_{MW} \left(1 - \frac{MW_{surr}}{MW_{target}}\right)^2 + w_{HC} \left(1 - \frac{HC_{surr}}{HC_{target}}\right)^2 + \\
& + w_{CN} \left(1 - \frac{CN_{surr}}{CN_{target}}\right)^2 + w_{YSI} \left(1 - \frac{YSI_{surr}}{YSI_{target}}\right)^2 + \\
& + w_{\mu} \left(1 - \frac{\mu_{surr}}{\mu_{target}}\right)^2 + w_{\rho} \left(1 - \frac{\rho_{surr}}{\rho_{target}}\right)^2 + \\
& + \frac{w_{DC}}{N_{DC}} \sum_{i=1}^{N_{DC}} \left(1 - \frac{T_{i,surr}}{T_{i,target}}\right)^2 + \frac{w_{IDT}}{N_{IDT}} \sum_{i=1}^{N_{IDT}} \left(1 - \frac{\ln\tau_{i,surr}}{\ln\tau_{i,target}}\right)^2 + \\
& + \frac{w_{LBV}}{N_{LBV}} \sum_{i=1}^{N_{LBV}} \left(1 - \frac{s_{Li,surr}}{s_{Li,target}}\right)^2
\end{aligned} \tag{5.1}$$

The assignment of weights values w_i will be object of Sections 5.4-5.5, as well as the decision of which properties should be considered (i.e. which w_i will be nonzero).

5.2 The optimization algorithm

The optimization routines presented in Section 2.2 should be compared in order to select the one that fits better for surrogates formulation.

The properties of the real fuel Jet A-1 are set as target*, and the performances of the different routines are compared in minimizing the objective function reported in Equation 5.1.

*See later Table 6.4 for details

The first approaches have been:

- the single use of `ga` (recall that it's able to select some species within the palette)
- the multiple use of `particleswarm` (being unable to select the species, it is run multiple times, each time activating a different species set. At the end the best result is selected)

with the constraint to have at least one species for each chemical family.

The comparison between these two trials (results are reported in Table 5.1) allowed to note that `particleswarm` was able to find a better minimum, but its necessity to be runned multiple times had a strong impact on the time required by the optimization.

So, the following idea was investigated: to split the optimization in two levels, as:

1. an initial, rough, optimization done by `ga`, considering only properties fast to be computed (like MW, H/C, CN...) but neglecting the curves in order to have a first selection of the species
2. a series of optimizations, considering all the properties, carried out through `fmincon`, `patternsearch` or `fminsearch`, that use the previous solution as first guess. Multiple runs are launched, each with different species 'activated', having set a limit of "species difference" (having a first guess, not all the combinations must be scanned). `particleswarm` has also been tested, but it was unable to exploit the previous solution.

5.2. The optimization algorithm

Routine	ga	particleswarm	ga+particleswarm
CPU time	1 min 50 s	9 min 23 s	2 min 14 s
Optimized composition	iC ₁₆ H ₃₄ : 11.06 nC ₁₀ H ₂₂ : 34.36 nC ₁₂ H ₂₆ : 27.07 nC ₇ H ₁₆ : 2.06 tmbenz: 25.45	iC ₁₆ H ₃₄ : 7.92 nC ₁₀ H ₂₂ : 10.26 nC ₁₂ H ₂₆ : 43.50 o-xylene: 38.32	iC ₁₆ H ₃₄ : 11.64 nC ₁₀ H ₂₂ : 41.96 nC ₁₂ H ₂₆ : 21.27 tmbenz: 25.12
f_{obj}	0.76807	0.73801	0.76113

Routine	ga+fminsearch	ga+fmincon	ga+patternsearch
CPU time	25 s	22 s	52 s
Optimized composition	iC ₁₆ H ₃₄ : 11.29 nC ₁₀ H ₂₂ : 37.96 nC ₁₂ H ₂₆ : 24.20 tmbenz: 22.67 o-xylene: 3.88	iC ₁₆ H ₃₄ : 7.92 nC ₁₀ H ₂₂ : 10.26 nC ₁₂ H ₂₆ : 43.50 o-xylene: 38.32	iC ₁₆ H ₃₄ : 7.92 nC ₁₀ H ₂₂ : 10.26 nC ₁₂ H ₂₆ : 43.50 o-xylene: 38.32
f_{obj}	0.76057	0.73801	0.73801

Table 5.1: Comparison of different optimization routines and routines combinations

This procedure allowed to speed up the optimization by about one order of magnitude.

It was noted that `fminsearch` failed in a significant number of optimizations, so it was not considered anymore.

On the other hand, `fmincon` and `patternsearch` were found pretty equivalent, even if sometimes one performed a little better than the other. For this

reason the chosen optimization strategy was the two-levels one, with multiple runs of both `patternsearch` and `fmincon` at the second level.

5.3 Validation of the optimization strategy

The developed strategy was tested on a few scenarios, by defining a known target and asking the optimizer to find a surrogate for that mixture (it is expected that the found surrogate coincides with the target).

For the moment, the following weights are considered in the objective function:

$w_{H/C}$	5	w_{ρ}	5	w_{DC}	1
w_{MW}	1	w_{μ}	1	w_{IDT}	1
w_{CN}	5	w_{YSI}	5	w_{LBV}	6

Table 5.2: Weights used in the objective function

These weights have been derived heuristically after some trials-and-errors by trying to keep all the contributions to the objective function similar.

Test #1

The first test is carried out using a 3-components mixture.

The optimization routine was able to find it again starting from its properties (considering the expected numerical inaccuracies): the results are reported in Tables 5.3 and 5.4.

5.3. Validation of the optimization strategy

	IC16H34	NC7H16	NC12H26	TMBENZ
x_{target}	0.40	-	0.35	0.25
$x_{surrogate}$	0.399075	0.00830	0.350203	0.249893

Table 5.3: Test #1 results - Mixtures

Property	Target value	Surr.value	ε
H/C	2.00	2.00	1.12E-09
MW	179.9	179.8	3.37E-07
CN	38.101	38.148	1.49E-06
μ	4.959	4.953	1.37E-06
YSI	62.276	62.261	6.01E-08
ρ	798.725	798.614	1.95E-08
DC			5.57E-07
IDT			7.22E-04
LBV			1.86E-04

Table 5.4: Test #1 results - Objective function

To show that the found point is actually the minimum it would be necessary to represent a function in more than 3 variables, which is impossible.

However, to visualize the minimum are reported in Figure 5.1 the trends of the objective function in the compositions space starting from the solution and changing one composition parametrically.

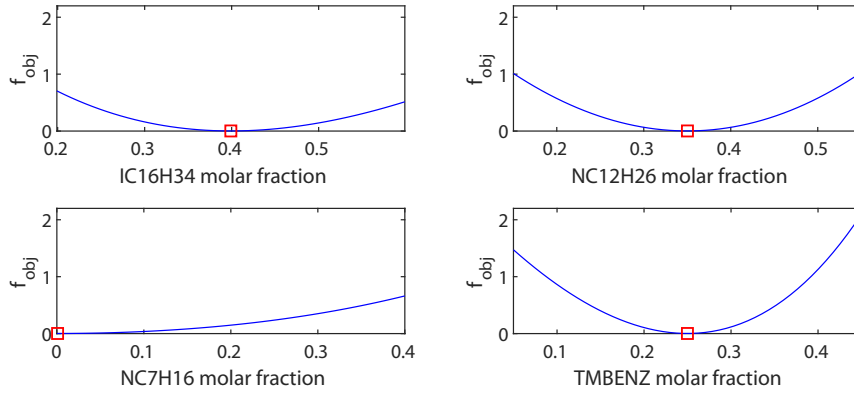


Figure 5.1: Representation of the objective function in the 4-dimensional space

Test #2

The second test is carried out using a 6-components mixture (increased complexity).

Also in this case the optimization routine was able to find the mixture again: the results are reported in Tables 5.5 and 5.6.

	iC ₁₆ H ₃₄	nC ₁₀ H ₂₂	nC ₁₂ H ₂₆	nC ₇ H ₁₆	tmbenz	o-xylene
x_{target}	0.40	0.10	0.20	0.05	0.15	0.10
x_{surr}	0.399986	0.085633	0.209243	0.058597	0.157368	0.089171

Table 5.5: Test #2 results - Mixtures

Like in the previous test, in Figure 5.2 are reported the trends of the objective function obtained by changing parametrically one composition, starting from the surrogate (represented by the red square).

5.3. Validation of the optimization strategy

Property	Target value	Surr.value	ε
H/C	2.000	2.002	1.26E-06
MW	172.2	172.324	5.21E-07
CN	35.492	35.522	7.32E-07
μ	4.622	4.631	4.52E-06
YSI	58.033	58.059	1.89E-07
ρ	793.615	792.821	1.00E-06
DC			8.71E-06
IDT			3.67E-04
LBV			2.84E-04

Table 5.6: Test #2 results - Objective function

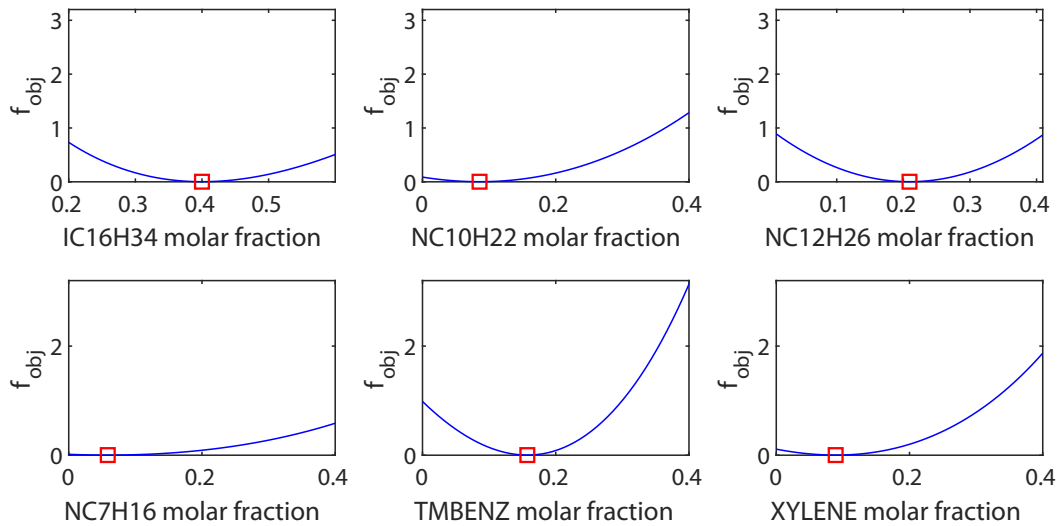


Figure 5.2: Representation of the objective function in the 6-dimensional space

Test #3

A further test is carried out using a 13-components mixture, in order to describe better the real fuel complexity. In this case, IDT and LBV are not considered, as metamodels were not developed for mixtures with this number of components. In addition, computation time is significantly increased respect to previous cases (by about two orders of magnitude).

	nC ₇ H ₁₆	nC ₁₀ H ₂₂	nC ₁₂ H ₂₆
x_{target}	0.03	0.12	0.08
x_{surr}	-	0.1418	0.0714
	nC ₁₆ H ₃₄	iC ₈ H ₁₈	iC ₁₂ H ₂₆
x_{target}	0.03	0.10	0.13
x_{surr}	0.0304	0.1253	0.1184
	iC ₁₆ H ₃₄	TMBENZ	C ₆ H ₅ C ₄ H ₉
x_{target}	0.03	0.10	0.07
x_{surr}	0.0272	0.0617	0.1041
	DECALIN	MCYC6	C ₁₀ H ₇ CH ₃
x_{target}	0.10	0.17	0.02
x_{surr}	0.1010	0.1777	0.0307
	TETRALIN		
x_{target}	0.02		
x_{surr}	0.0103		

Table 5.7: Test #3 results - Mixtures

It's possible to see that, even if the composition is not retrieved as accurately as in previous cases (Table 5.7), the properties are however well described

(Table 5.8). Note that the "species difference" parameter between the two optimization levels can be decreased, speeding up the optimization at the cost of a little lower accuracy in properties estimation.

Property	Target value	Surr.value	ε
H/C	1.933	1.933	6.51E-11
MW	138.22	138.231	6.79E-09
CN	38.939	38.939	1.31E-12
μ	2.994	2.994	3.10E-11
YSI	68.335	68.335	2.40E-13
ρ	788.120	788.129	1.26E-10
DC			8.93E-08

Table 5.8: Test #3 results - Objective function

5.4 Selection of properties to be optimized

The framework developed up to now is able to optimize 9 different properties of the jet fuel surrogate: molecular weight, H/C ratio, cetane number, viscosity, yield sooting index, density, distillation curve, ignition delay times curve and laminar burning velocity curve.

However, since the formulation of a surrogate is carried out in a phase where this amount of information is seldom experimentally available, this section is focused on the selection of a minimal set of properties to be optimized that allows to have an overall acceptable surrogate. In other words, the possibility to accurately describe some properties even when they are not directly

optimized is investigated.

In order to study the behavior of the optimizer, the same three test mixtures used in Section 5.3 are used and a 6-components species palette to formulate the surrogate.

5.4.1 Selection of two basic properties

The optimization of density and H/C ratio is used as "base case", as these two properties are commonly available and in any case are easy to be determined experimentally. The optimizer is run with only ρ and H/C to be optimized,

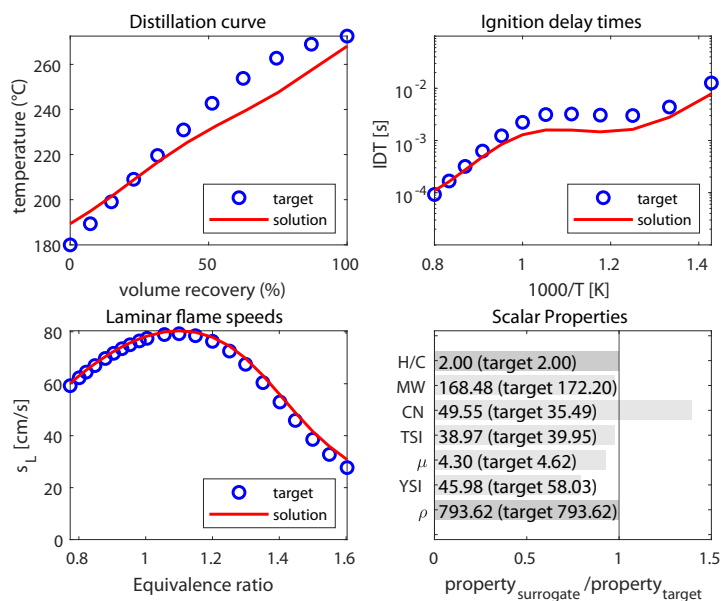


Figure 5.3: Properties of the surrogate for test mix #2 obtained optimizing ρ and H/C

obtaining mixtures that effectively represent the two properties but do not represent well any other properties (in Figure 5.3 the obtained results for

test mixture #2 are reported: the target and obtained properties are plotted, while for scalar properties are reported the ratios between the obtained and the target property. In an ideal situation, they should be close to 1)

5.4.2 Addition of a third property

It is evident that only two properties are not sufficient to efficiently describe the fuel as a whole.

So, several tests are carried out by adding one other property to be optimized: all the 7 remaining properties are considered, one at time, for the three test mixtures.

The average[†] errors ε on all properties defined in Section 5.1 are compared in Figure 5.4: it is reported the ratio between ε computed optimizing the two basic properties and ε obtained optimizing three properties (i.e. when the ratio is high the addition of the third property carries a significant improvement in the accurate description of the target).

It is chosen as third property to be optimized the cetane number, as it gave a good improvement of results in all the tests. Note that YSI gave similar results, but CN is preferred as it's easier to be retrieved as target.

The properties of the surrogate formulated by optimizing ρ , H/C and CN are reported in Figure 5.5, with the same graphical format of Figure 5.3. The comparison of the two figures allows to have a visual representation of the

[†]Here and in the next sections, having to compare errors with different orders of magnitude, it is preferred to use geometric means instead of the common arithmetic means.

Chapter 5. Development of an optimization strategy for surrogates formulation

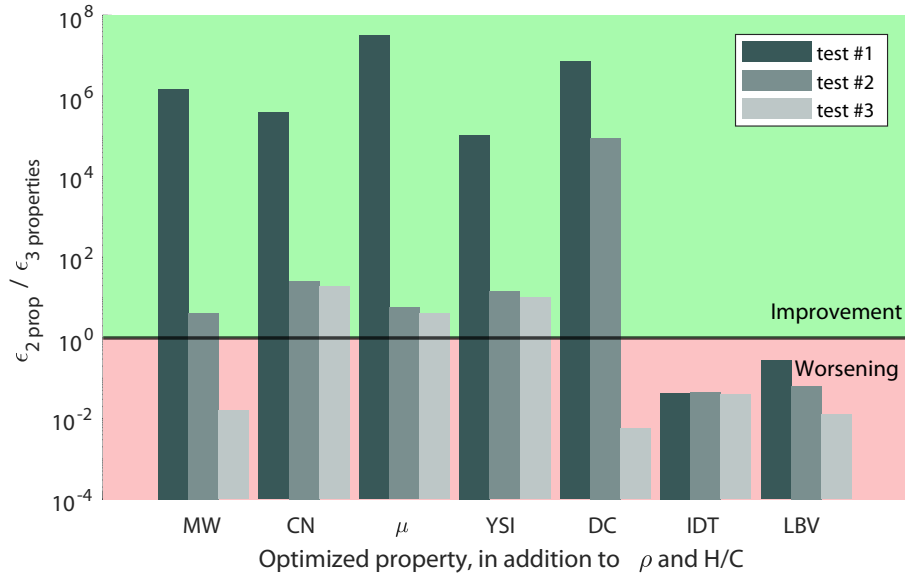


Figure 5.4: Comparison of ϵ between surrogates obtained by optimizing 2 and 3 properties

improvement that the third property can give.

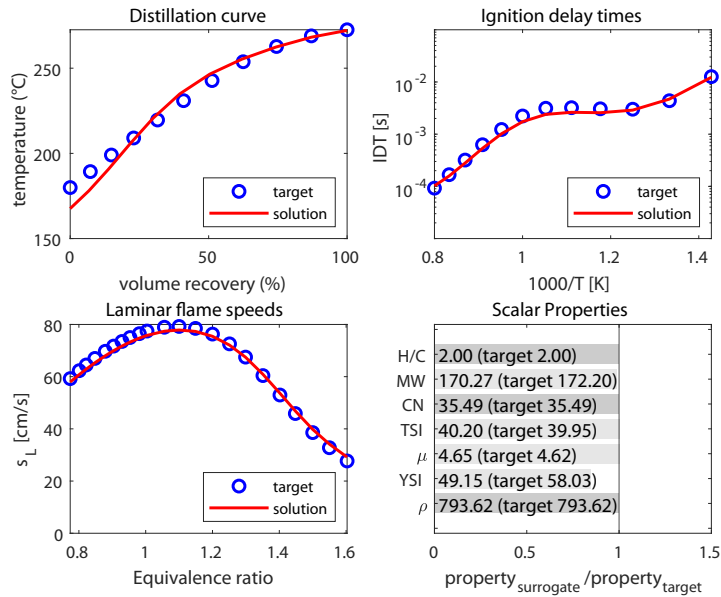


Figure 5.5: Properties of the surrogate for test mix #2 obtained optimizing ρ , H/C and CN

5.4.3 Addition of a fourth property

Starting from a base of ρ , H/C and CN, other optimizations are run adding further properties to be optimized.

In Figure 5.6 the results obtained in all the tests conducted are summarized. On the rows are reported the tests, identified by the set of properties optimized, while on the columns are reported the errors with which are described the different properties (it is reported the average value between the three test mixtures).

More detailed data, differentiated on the three tests, are reported in Appendix B). The properties that are optimized are drawn with a striped pattern (it is expected that in these cells the error has a low value).

The plot is meant to be read row by row: if a set of optimized properties is able to describe the whole fuel, the corresponding row will be mostly characterized by green cells. If instead red or orange cells are present on the row, it can be seen as a warning that some properties are not well described.

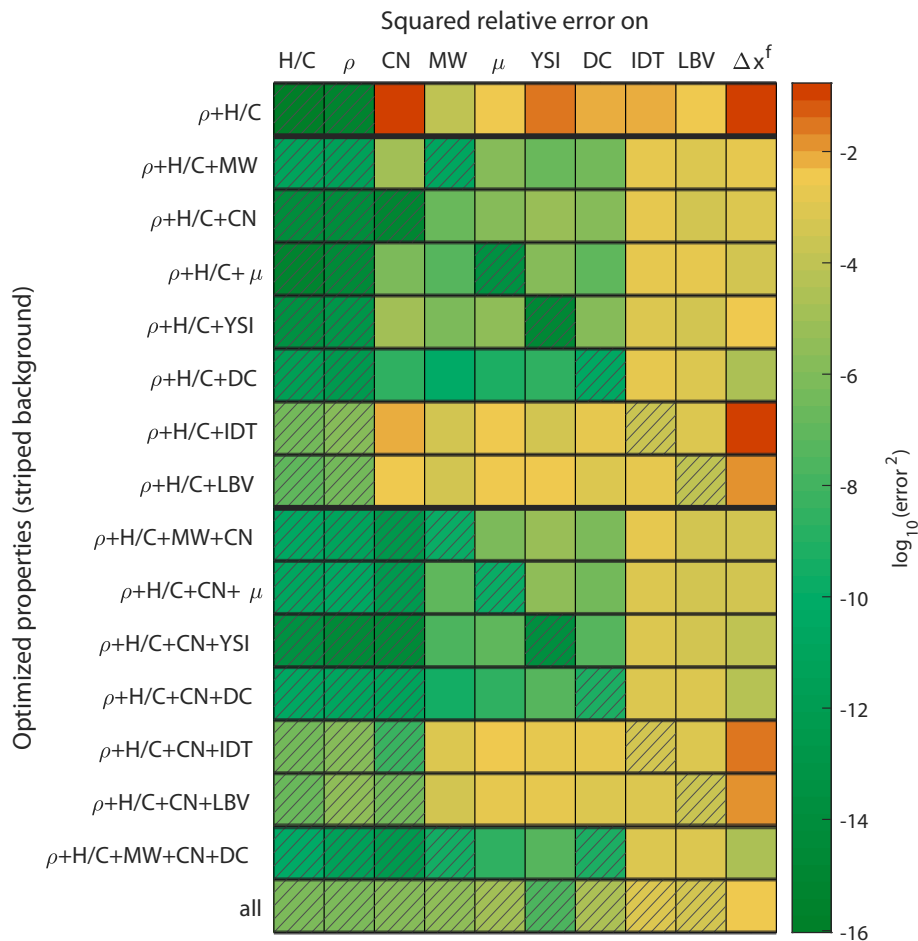


Figure 5.6: ε on each property (on the columns) for each set of properties optimized (on the rows) - reported as average on the three test mixtures. An additional data on composition is reported as average Δx on families (test #3 is not considered in this last column as the species palette is smaller than the target).

5.4.4 Analysis of results

From Figure 5.4 it's possible to see that when the test mixture #3 is considered, results are always worse than with other mixtures: this can be explained by its composition -13 species- that the optimizer's palette of 6 species reproduces with difficulty. This is particularly evident considering the distillation curve, that otherwise would have been a better candidate for third property to be optimized.

Regarding the addition of a fourth property, the mixture molecular weight, the viscosity and the YSI behaved similarly, while the distillation curve performed a little better: being the DC relatively easy to be found in literature and required for later tests, when it is available it could be a good idea to include it among the optimized properties, having in mind that, due to what seen just above, the species palette should be wide enough.

A peculiar behavior arises from the ignition delay time and laminar burning velocity curves: their inclusion in the optimized properties set causes a clear decrease in performances on all the other properties. This could be explained by considering the fact that in the vast space of mixtures compositions exist many points that can reproduce the same curve, even with clearly different compositions (refer to the Δx^{family} column of Figure 5.6 when IDT or LBV are optimized).

However, from the same figure is possible to see that IDT and LBV curves are described with the same accuracy even when they are not optimized, and

that accuracy can be considered satisfying, being $\varepsilon_{IDT}, \varepsilon_{LBV}$ in the order of 1%. This can be due to the fact that the properties are not completely independent one from the other (e.g. cetane number is correlated to ignition, so indirectly to IDT).

A last test was carried out optimizing all the available properties, to have an idea of the best result that can be achieved using this tool.

5.5 Selection of optimization weights

From the results just obtained, it's possible to have an idea of how important is each property considered. In particular:

- DENSITY, H/C RATIO and CETANE NUMBER alone are able to guide the optimizer to the right direction: their weight should be relevant.
- MOLECULAR WEIGHT, VISCOSITY and YIELD SOOTING INDEX should have a comparable weight.
- DISTILLATION CURVE, when available, can have a positive impact on the surrogate quality.
- IDT and LBV curves do not contribute significantly to the surrogate quality so they should not be considered in the optimization.

Based on this, the previous weights (Table 5.2) are replaced by the ones proposed here in Table 5.9 (obviously, if the property is not included in the

optimization its weight is automatically set to zero):

$w_{H/C}$	10	w_{MW}	5	w_{DC}	1
w_{ρ}	10	w_{μ}	5	w_{IDT}	0
w_{CN}	10	w_{YSI}	5	w_{LBV}	0

Table 5.9: Proposed weights to be used in the objective function

Using this weights set, an optimization considering all the properties is run, and the optimized obj. function for the three test mixture is composed as:

	f_{obj} contribution (i.e. $w_i \cdot \varepsilon_i$)		
	test 1	test 2	test 3
H/C	7.44E-16	1.64E-14	4.87E-4
ρ	1.04E-16	9.69E-16	1.44E-4
CN	1.79E-16	3.97E-18	2.76E-6
MW	1.03E-15	1.22E-13	6.50E-4
μ	2.57E-15	2.26E-15	3.94E-4
YSI	3.00E-14	3.40E-15	1.03E-7
DC	6.99E-17	1.24E-13	9.40E-3

Table 5.10: Composition of the objective function using the proposed weight set

It's possible to see that when the surrogate fits well the target, the single contributions may differ by some orders of magnitude. This is not to be taken as a symptom that some properties are unbalanced, unless the error becomes relevant (in the order of some points %).

5.6 Summary

In this chapter the optimizer on which the surrogate formulation procedure is based has been developed.

The importance of the different properties has been studied and the parameters have been tuned.

In addition, the possibility to consider only a small set of known properties to describe the whole fuel has been investigated, and a minimal set of properties is proposed: this can help to decide which experiments should be conducted at an early stage on the real fuel to retrieve those properties.

At this point the developed tool is tested and ready to be used.

Chapter 6

Application to real fuels

Since the framework for the formulation of a fuel surrogate is now developed, in this chapter it is used to construct surrogates for two real fuels, in order to verify its behavior.

In particular are searched surrogates for the POSF-4658 fuel (a fuel used to carry out tests regarding the JET A class of fuels) and for JET A-1 (the most widespread jet fuel worldwide).

Several surrogates are developed, in order to show the impact of the species palette and the number of compounds used to build up the surrogate on the final result.

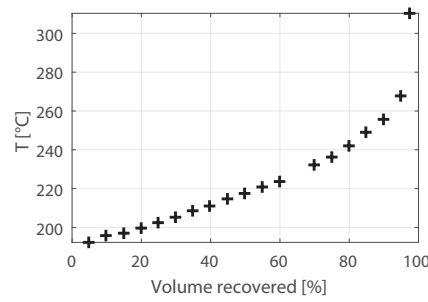
Moreover, the surrogates of POSF-4658 formulated by the framework are compared with other surrogates available in literature and derived by different authors. This has the purpose to show the validity of the tool presented here.

6.1 A surrogate for POSF-4658

The following properties are selected as target for the optimizer:

Property	Value	Source
H/C ratio	1.957	(35)
Cetane number	47.1	(35)
Density (at 298.15K)	799.38 kg/m^3	(36)
Molecular weight	142 $kg/kmol$	(35)
Viscosity (at 273.15K)	2.3878 cP	(36)
YSI	75.5	(37)

Distillation curve



(38)


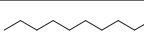
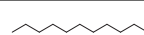
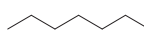
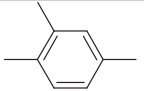
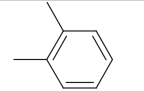
Table 6.1: Properties of POSF-4658 fuel

According to what derived in the previous chapter, the properties to be optimized are H/C , density, cetane number and distillation curve.

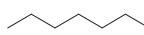
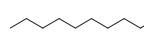
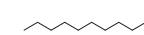
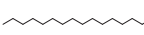
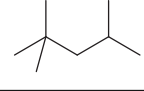
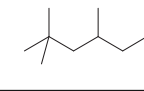

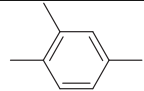
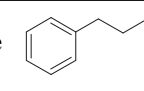
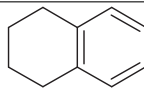
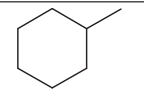
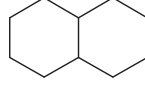
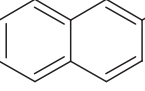
6.1. A surrogate for POSF-4658

The number of species that will form the surrogate can be constrained. Four different optimizations are run:

- with a maximum of 3 or 6 species selected from the following palette

iso-cetane $iC_{16}H_{34}$		n-decane $nC_{10}H_{22}$		n-dodecane $nC_{12}H_{26}$	
n-heptane nC_7H_{16}		trimethylbenzene TMBENZ		o-xylene XYLENE	

- with a maximum of 6 or 10 species selected from the following palette

n-heptane nC_7H_{16}		n-decane $nC_{10}H_{22}$		n-dodecane $nC_{12}H_{26}$	
n-cetane $nC_{16}H_{34}$		i-octane iC_8H_{18}		i-dodecane $iC_{12}H_{26}$	
i-cetane $iC_{16}H_{34}$		trimethylbenzene TMBENZ		butylbenzene $C_6H_5C_4H_9$	
tetralin TETRA		methylcyclohexane MCYC6			
decalin DECALIN		α -methylnaphthalene $C_{10}H_7CH_3$			

The surrogates obtained and their properties are reported in the following tables and figures.

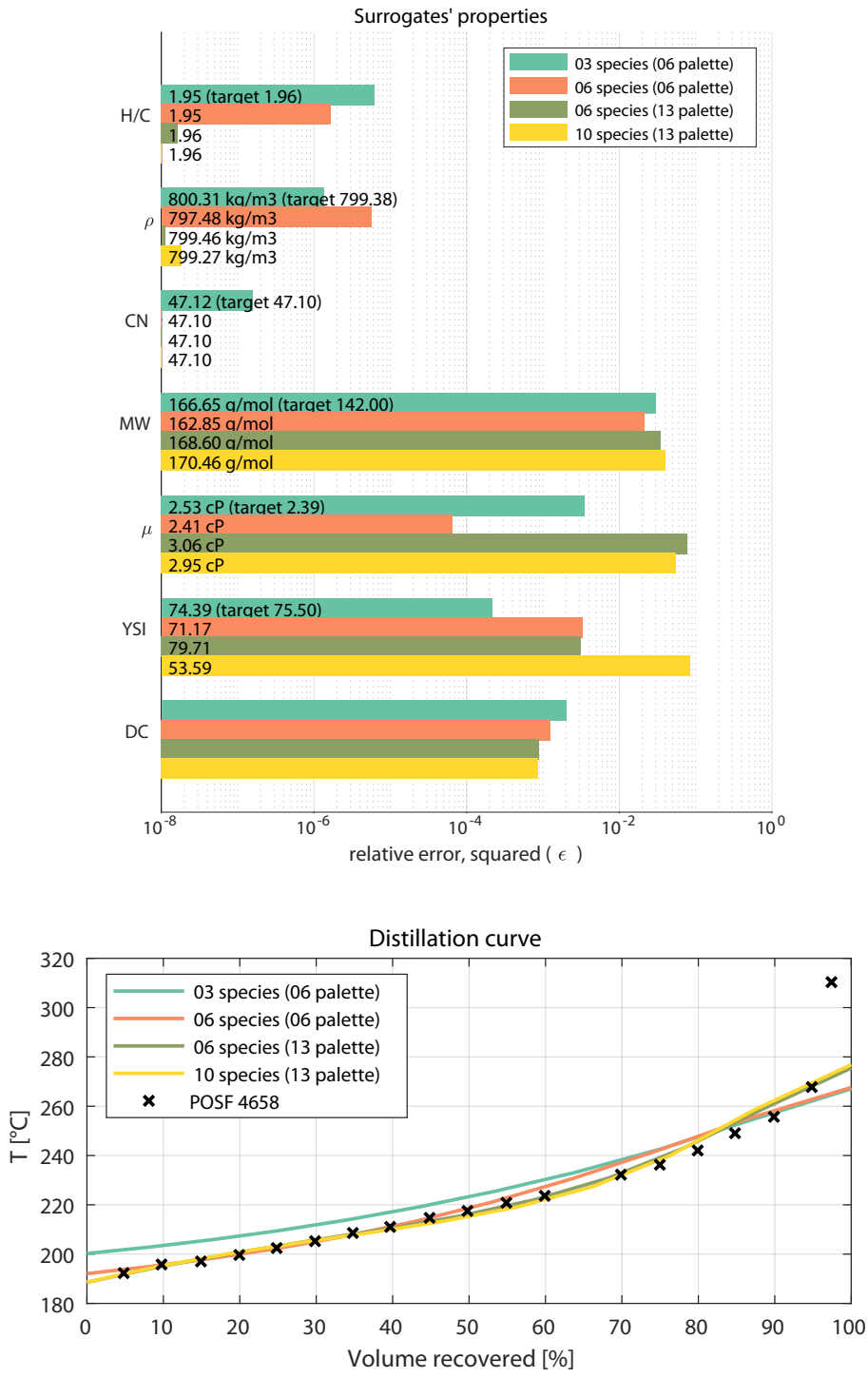


Figure 6.1: Properties of POSF-4658 surrogates

	6-species palette		13-species palette	
Max # of species	3	6	6	10
nC ₁₀ H ₂₂	-	0.1090	-	-
nC ₁₂ H ₂₆	0.4513	0.3524	0.1982	0.2143
nC ₁₆ H ₃₄	-	-	0.1444	0.1277
iC ₈ H ₁₈	-	-	0.0374	0.0122
iC ₁₂ H ₂₆	-	-	0.3700	0.3100
iC ₁₆ H ₃₄	0.2272	0.2223	-	0.0596
MCYC6	-	-	-	0.0273
DECALIN	-	-	0.0982	0.1008
XYLENE	-	0.0521	-	-
TMBENZ	0.3215	0.2643	-	-
C ₆ H ₅ C ₄ H ₉	-	-	-	0.0009
TETRA	-	-	-	0.1415
C ₁₀ H ₇ CH ₃	-	-	0.1517	0.0058
Obj. function	0.002083	0.001335	0.000884	0.00086

Table 6.2: Composition of POSF-4658 surrogates (one per column)

It is possible to notice that the transition from 3 to 6 species allows a general improvement of performances. Among the 6-components surrogates, the choice of a wider species palette improves the description of the distillation curve at the expense of the other scalar properties.

The further addition of species does not carry any significant improvement. Considering the fact that in the surrogate formulation the complexity should be kept as low as possible, a number of species around 6 can be recommended.

Ignition delay times and laminar burning velocities were not included in the objective function, as in Chapter 5 has been shown that their inclusion does not carry relevant information. However, it is important to check afterwards that these two properties are predicted with a reasonable accuracy.

So, detailed OpenSMOKE++ simulations are run, using the *CRECK_2003_TOT* kinetic mechanism (39).

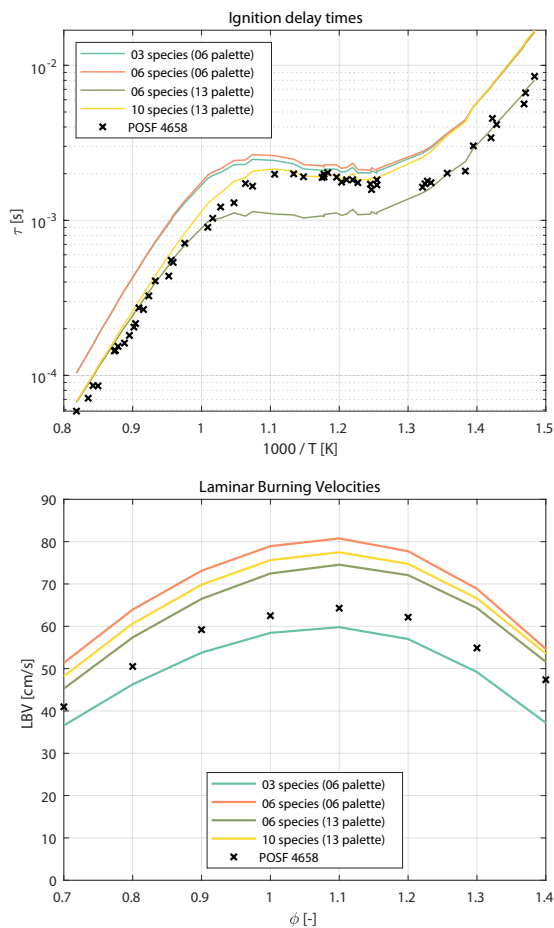


Figure 6.2: Ignition delay times and laminar burning velocities of POSF-4658 (35, 40) and of derived surrogates

Conditions of IDT: 16-25 bar. Conditions of LBV: 400 K, 1 bar.
 IDT points are scaled to a uniform pressure of 22 bar assuming a conversion formula of $\tau(22 \text{ bar}) = \tau(P) \cdot P/22 \text{ bar}$.

6.2 Comparison with surrogates available in the literature

The surrogates developed in the previous section with a maximum of 6 species are now compared with these surrogates available in the scientific literature:

- n-decane 0.4267, iso-octane 0.3302, toluene 0.2431 by Dooley et al. (35)
- n-dodecane 0.3844, iso-cetane 0.1484, methyl-cyclohexane 0.2336, toluene 0.2336 by Kim et al. (41)
- n-dodecane 0.2897, iso-cetane 0.1424, decalin 0.3188, toluene 0.2491 by Kim et al. (41)

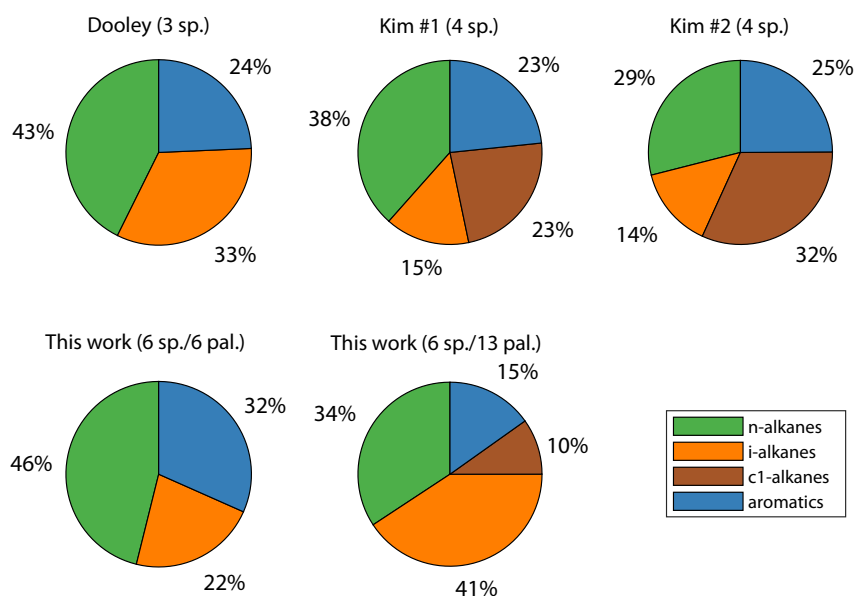


Figure 6.3: Molar composition of POSF-4658 surrogates by families

The properties of such surrogates, computed according to the mixing rules

presented in Chapter 2, are the following:

	Dooley	Kim #1	Kim #2	This work (6 palette)	This work (13 palette)	<i>POSF-4658</i> (target)
ρ	751.82	789.09	832.56	797.48	799.46	799.38
H/C	2.01	1.97	1.88	1.95	1.96	1.96
CN	46.96	47.17	47.62	47.10	47.10	47.10
MW	120.60	143.27	148.34	162.85	168.60	142.00
μ	0.98	2.07	2.56	2.41	3.06	2.39
YSI	19.21	21.58	32.63	71.17	79.71	75.50

Table 6.3: Comparison of POSF-4658 surrogates' properties
 Boldface numbers represent optimized properties

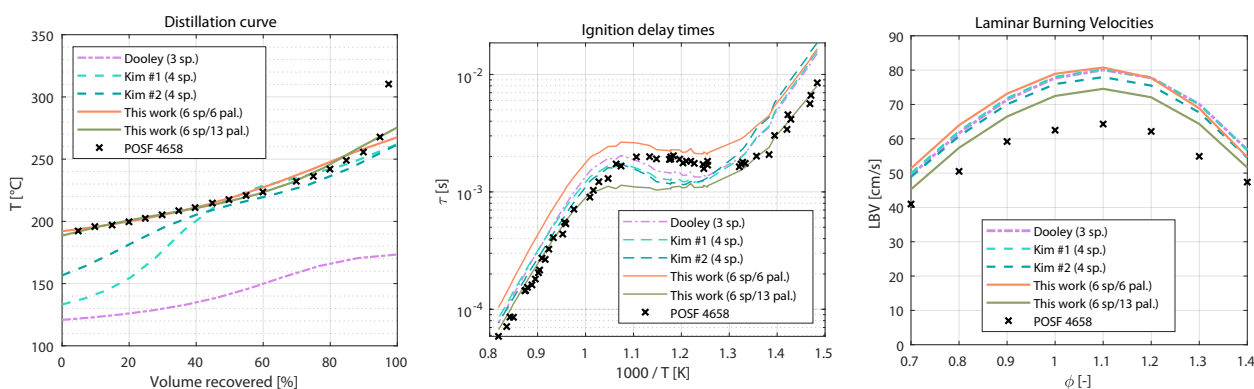


Figure 6.4: Comparison of POSF-4658 surrogates' curves

Dooley's surrogate has been developed optimizing a derived cetane number (DCN), the H/C ratio, the molecular weight and the threshold sooting index (TSI), with a similar meaning of YSI. On the other hand, Kim's surrogates have been developed optimizing CN, H/C, MW, ρ , μ , the lower heating value (LHV), the surface tension and the distillation curve.

6.2. Comparison with surrogates available in the literature

It is possible to see that on some properties the performances are similar (like H/C, CN), while on others (like density, sooting index and distillation curve) the surrogates proposed in this work perform better. MW, on the opposite, was not optimized in this work, so it is better captured by literature surrogates.

The presence, in the surrogates presented here, in significant quantities of high-boiling species, like n- and iso-cetane, or aromatics heavier than toluene may cause a worsening in molecular weight representation but on the other side allows an efficient description of the distillation curve, that in the considered literature surrogates completely lacks. The choice of a wide species palette reveals here its impact.

It must be noted, however, that despite a smaller number of species, the literature surrogates are able to capture the ignition delay times curve with more accuracy than the ones developed here, while for laminar burning velocities the performances are similar.

6.3 A surrogate for Jet A-1

To produce a surrogate for JET A-1 fuel, the target for the optimizer is now changed as follows:

Property	Value
H/C ratio	1.94
Cetane number	47.0
Density (at 298.15K)	801 kg/m^3
Molecular weight	154 $kg/kmol$
Viscosity (at 298.15K)	2.6672 cP
YSI	60.0

Distillation curve

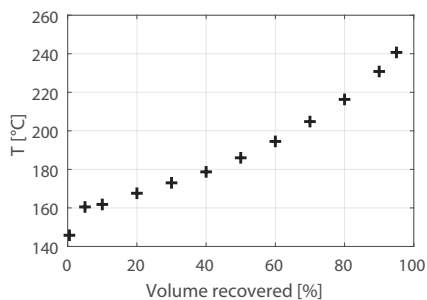


Table 6.4: Properties of Jet A-1 - Source (42)

The same strategy followed for POSF-4658 is applied also to JET A-1 (a surrogate of maximum 3 species, two of max. 6 species, changing the palette, and one of max. 10 species), obtaining the four surrogates reported here in Table 6.5 with properties reported in Figures 6.6-6.7.

The behavior of the optimizer is similar to the POSF-4658 case: the best number of species is 6, being the 3-species surrogate not completely adequate and the 10-species surrogate not carrying any appreciable improvement re-

6.3. A surrogate for Jet A-1

	6-species palette		13-species palette	
Max # of species	3	6	6	10
nC ₇ H ₁₆	-	0.05425	-	-
nC ₁₀ H ₂₂	0.48173	0.39631	0.37161	0.26653
nC ₁₂ H ₂₆	-	0.04633	-	0.08585
iC ₈ H ₁₈	-	-	-	0.00279
iC ₁₂ H ₂₆	-	-	0.08482	0.04675
iC ₁₆ H ₃₄	0.16888	0.15615	0.06565	0.07596
MCYC6	-	-	0.19675	0.19235
DECALIN	-	-	0.17239	0.16386
XYLENE	0.34939	0.34401	-	-
TMBENZ	-	0.00294	-	0.12635
C ₁₀ H ₇ CH ₃	-	-	0.10878	0.03956
Obj. function	0.005872	0.005074	0.000356	0.000350

Table 6.5: Composition of Jet A-1 surrogates (one per column)

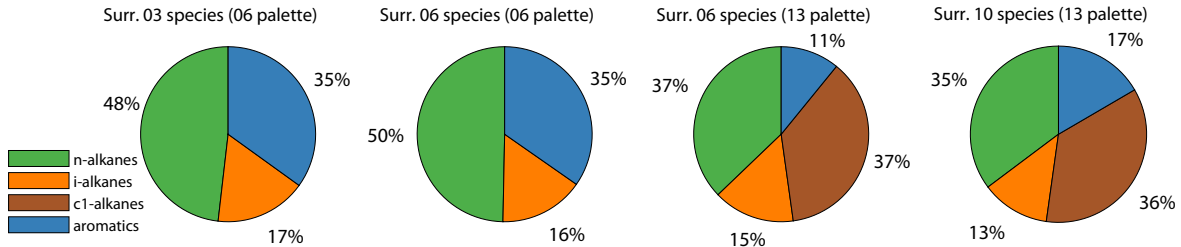


Figure 6.5: Molar composition of Jet A-1 surrogates by families

spect to the 6-species one (only a small increase in the LBV curve). Again, the choice of a smaller palette allows a better description of the scalar properties but a worse match of the curves (with the exception of the LBV curve). It must be noted that the viscosity isn't well captured in any case: a wider species palette, rich in viscous species, could limit this problem.

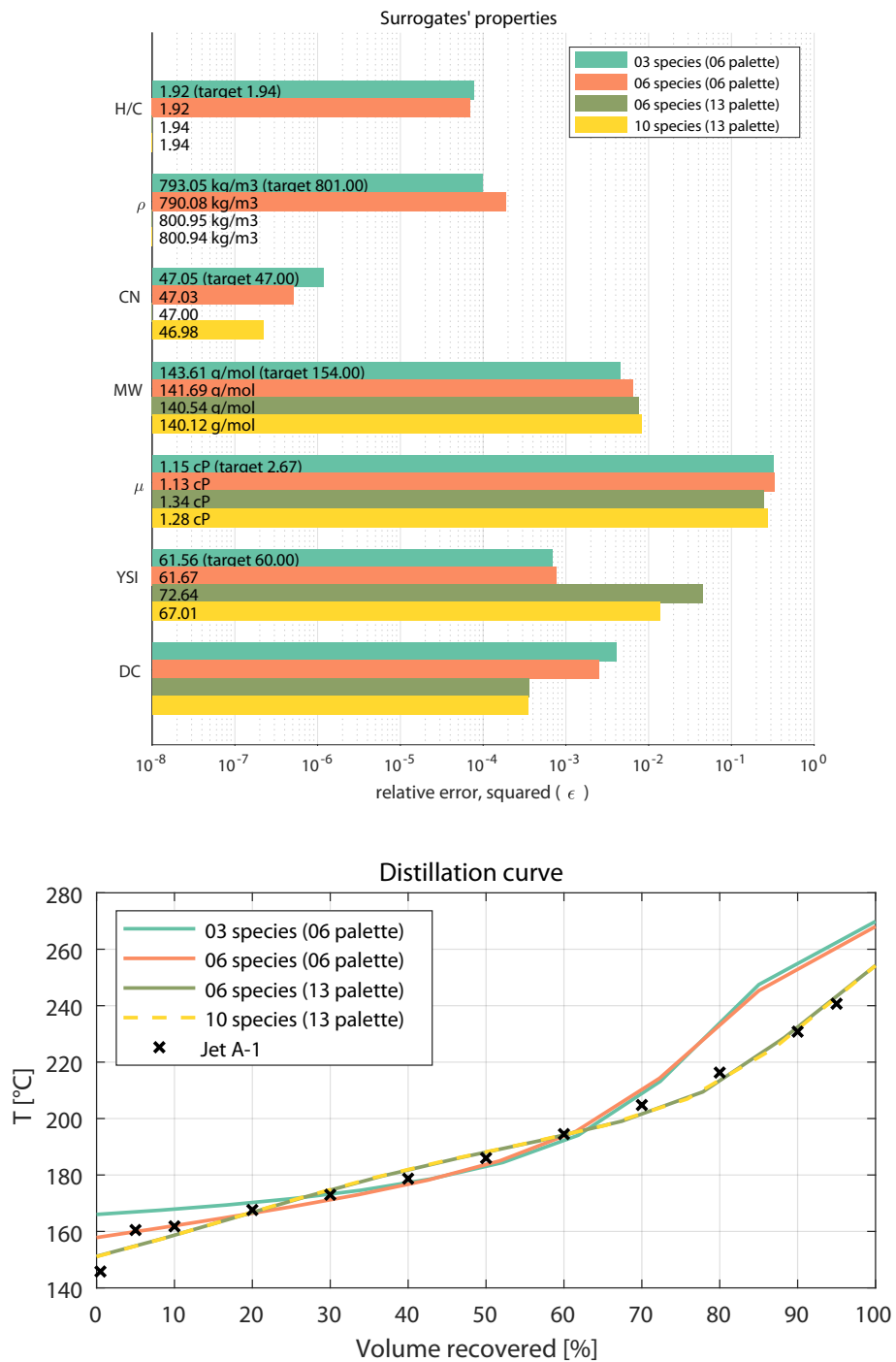


Figure 6.6: Properties of Jet A-1 surrogates

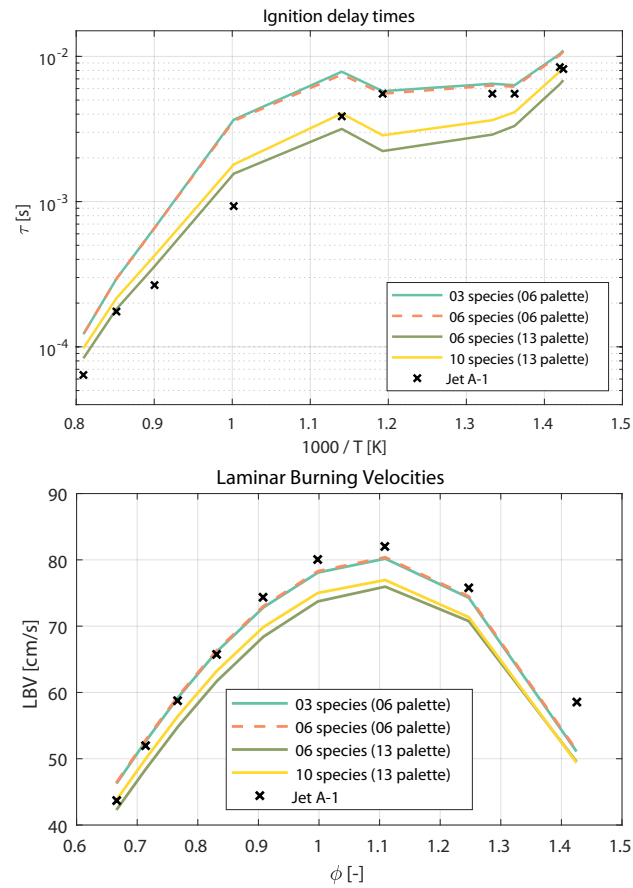


Figure 6.7: Ignition delay times and laminar burning velocities of Jet A-1 (43, 44) and of surrogates

Conditions of IDT: 13-16 bar. Conditions of LBV: 473 K, 1 bar.

Nevertheless, the two 6-species surrogates can be considered acceptable, being a perfect correspondence impossible, given that even the real fuels do not coincide with the targets used.

6.4 Summary

In this chapter the developed `Matlab` framework is applied on two real cases: the fuels POSF-4658 and JET A-1. The surrogates produced has been considered satisfactory, and their validity has been assessed by comparison with other surrogates available in the scientific literature.

For this reason is now possible to publish the computing tool.

Chapter 7

Conclusions and future developments

The aim of this work was to develop and test a **Matlab**[®] framework to support the selection, analysis and screening of jet fuels surrogates.

The framework is able to formulate a surrogate imposing that some properties trace a given set of data. Here nine different properties have been implemented to characterize a fuel: the code has the objective of computing a mixture whose properties are as similar as possible to the data supplied by the user. The user has also the duty to indicate a list of chemical compounds among which the program will choose the species used to build the surrogate.

For two of the considered properties, the ignition delay times and laminar burning velocities, the evaluation using a numerical simulation revealed to be excessively time consuming: two specific metamodels have been derived in

order to have a quick approximation of these two properties and allowing their implementation in the iterative formulation of the surrogate. The subsequent tests showed how these properties are not strictly necessary to formulate a good surrogate fuel, allowing one to neglect them with the awareness that this won't compromise the result.

The formulation procedure is implemented as an optimization problem, with the objective of minimizing the difference between the properties of the target fuel and the ones of the surrogate.

The resulting program is considered satisfactory, however are present improvement margins: in particular here have been implemented simple mixing rules for most of the properties covered (e.g. cetane number, sooting index, viscosity). It would be possible to consider more sophisticated mixing rules that are available in the literature.

Another relevant point is the possibility to implement other properties beyond the nine considered here: some examples can be the heating value, the surface tension, the flash point...

A remark is necessary: it is not wise to take for granted the idea that the addition of properties will necessarily improve the result. In this work it was faced this aspect, showing that some properties may mislead the optimizer. Moreover, additional properties will probably lead to a slowing down of the routine.

Another aspect to consider is the choice of a single objective function: the results are strongly dependent on its parameters and functional shape.

A final detail is the data provided by the user: if it is not expected that experimental data about the fuel will become optional, on the other side the choice of the species palette can be more automated in the future.

Appendix A

Kriging model for IDT

The following pages contain the parameters derived for all reduced models (each reported in a column) $\tau = \tau(T, \phi, \bar{x})$ considering 6 components.

Recall that ϑ parameters denotes the physical importance of each variable, while λ parameter indicates how much the regression tends to an interpolation (this happens as $\lambda \rightarrow 0$).

$-\ln(\textit{Likelihood})$ is the objective function for the optimization procedure.

Pressure [bar]	1	2	3	5	10
$\log_{10} \vartheta(T)$	0.8883	0.9083	0.9283	0.9212	0.9062
$\log_{10} \vartheta(\phi)$	-1.2504	-1.2304	-1.2504	-1.2433	-1.2511
$\log_{10} \vartheta(x_{IC16H34})$	-1.2517	-1.2317	-1.2517	-1.2446	-1.2299
$\log_{10} \vartheta(x_{NC10H22})$	-1.9388	-1.9588	-1.9388	-1.9631	-1.9546
$\log_{10} \vartheta(x_{NC12H26})$	-1.2424	-1.2624	-1.2824	-1.2613	-1.2294
$\log_{10} \vartheta(x_{NC7H16})$	-2.7400	-2.7600	-2.7400	-2.7471	-2.8261
$\log_{10} \vartheta(x_{TMBENZ})$	-0.1662	-0.1862	-0.2062	-0.1833	-0.1855
$\log_{10} \vartheta(x_{XYLENE})$	-0.4017	-0.3817	-0.4017	-0.4088	-0.4544
λ	3.54E-04	3.49E-04	5.37E-04	2.50E-04	4.89E-04
$-\ln(\text{Likelihood})$	-176.5193	-148.7672	-153.8752	-157.0412	-147.9075
R^2 on fit points	0.999763	0.99921	0.999239	0.999659	0.999168
Maximum and average errors of $\ln(\tau)$ on fit points.					
Absolute error, max	1.1E-01	8.1E-02	3.9E-02	2.9E-02	5.6E-03
Absolute error, mean	1.1E-02	7.7E-03	4.3E-03	1.6E-03	6.9E-04
Relative error, max	1.2E-01	1.3E-01	1.4E-01	1.1E-01	2.0E-01
Relative error, mean	2.7E-02	3.1E-02	3.4E-02	2.3E-02	3.5E-02

Appendix A. Kriging model for IDT

Pressure [bar]	20	30	50	70	100
$\log_{10} \vartheta(T)$	0.9159	0.9096	0.8537	0.8480	0.7990
$\log_{10} \vartheta(\phi)$	-1.2803	-1.3326	-1.3639	-1.4183	-1.4499
$\log_{10} \vartheta(x_{IC16H34})$	-1.1677	-1.1446	-1.1751	-1.1387	-1.1341
$\log_{10} \vartheta(x_{NC10H22})$	-1.9311	-1.9473	-1.9267	-1.9328	-1.9919
$\log_{10} \vartheta(x_{NC12H26})$	-1.2332	-1.1797	-1.2159	-1.2057	-1.2404
$\log_{10} \vartheta(x_{NC7H16})$	-2.8214	-2.8707	-2.7934	-2.8160	-2.8999
$\log_{10} \vartheta(x_{TMBENZ})$	-0.1514	-0.1263	-0.1375	-0.1696	-0.2677
$\log_{10} \vartheta(x_{XYLENE})$	-0.4880	-0.4970	-0.6034	-0.6472	-0.7629
λ	1.94E-04	2.45E-04	1.79E-04	7.81E-05	9.40E-05
$-\ln(Likelihood)$	-185.8982	-160.5696	-149.2454	-196.4044	-190.3654
R^2 on fit points	0.99984	0.999787	0.999846	0.999964	0.999955
Maximum and average errors of $\ln(\tau)$ on fit points.					
Absolute error, max	3.3E-03	6.9E-03	3.9E-03	2.1E-03	6.5E-03
Absolute error, mean	1.9E-04	2.3E-04	2.5E-04	1.8E-04	3.0E-04
Relative error, max	9.2E-02	9.6E-02	1.2E-01	4.6E-02	8.3E-02
Relative error, mean	1.6E-02	2.1E-02	2.1E-02	1.1E-02	1.4E-02

Appendix B

Data about the optimizer behavior respect to the optimized properties

The following tables are the extended version of Figure 5.6: the sets of optimized variables are reported the rows, while on columns are reported the errors ε on each variable, differentiated for the three test mixtures.

I.e. considering a single row, it is possible to retrieve on the columns the accuracy with which each property is described.

Appendix B. Data about the optimizer behavior respect to the optimized properties

	MW			HC			CN			mu			YSI		
	test1	test2	test3	test1	test2	test3	test1	test2	test3	test1	test2	test3	test1	test2	test3
HC+rho	9E-4	2E-6	4E-4	8E-16	2E-16	6E-18	6E-2	2E-1	4E-1	7E-4	1E-2	2E-2	3E-2	8E-3	3E-2
HC+rho+MW	2E-14	2E-13	2E-6	9E-16	6E-13	1E-6	3E-13	6E-2	1E-1	1E-13	9E-4	3E-2	5E-14	1E-5	2E-2
HC+rho+CN	2E-13	1E-5	2E-3	7E-14	5E-15	3E-15	7E-17	1E-14	4E-15	6E-13	6E-4	6E-3	6E-12	1E-2	1E-2
HC+rho+mu	1E-16	2E-4	5E-3	7E-17	1E-14	4E-16	2E-16	5E-3	4E-1	3E-16	1E-12	9E-14	6E-15	2E-2	2E-2
HC+rho+YSI	2E-12	3E-5	3E-3	7E-15	9E-13	2E-14	7E-11	2E-3	7E-3	1E-11	9E-4	6E-3	2E-16	2E-14	6E-15
HC+rho+DC	2E-15	5E-13	1E-3	3E-16	2E-15	2E-5	4E-15	4E-11	1E-1	5E-15	2E-12	4E-2	2E-14	8E-11	1E-2
HC+rho+IDT	6E-4	2E-5	3E-3	1E-6	1E-7	6E-7	7E-3	3E-2	7E-4	3E-3	2E-3	4E-3	1E-4	5E-3	1E-4
HC+rho+LBV	3E-5	7E-4	1E-2	1E-6	7E-9	5E-8	5E-4	9E-4	2E-1	2E-4	2E-3	9E-2	6E-5	8E-3	4E-2
HC+rho+MW+CN	1E-13	2E-12	2E-5	4E-14	7E-14	9E-6	1E-14	6E-16	3E-9	4E-13	8E-4	3E-3	3E-12	6E-3	7E-3
HC+rho+CN+mu	1E-12	3E-6	7E-4	3E-13	5E-14	9E-7	1E-14	1E-14	4E-9	3E-12	5E-12	4E-7	2E-11	4E-4	9E-3
HC+rho+CN+YSI	5E-17	2E-5	4E-3	8E-18	4E-12	2E-12	2E-16	6E-13	1E-15	2E-16	5E-4	2E-2	6E-16	6E-14	7E-14
HC+rho+CN+DC	1E-13	8E-13	6E-4	5E-14	2E-14	2E-4	7E-15	2E-14	4E-6	4E-13	1E-12	2E-2	4E-12	3E-10	1E-1
HC+rho+CN+IDT	8E-4	4E-4	4E-3	8E-7	3E-7	5E-7	2E-8	2E-8	1E-9	3E-3	1E-3	7E-3	8E-3	6E-3	1E-4
HC+rho+CN+LBV	2E-5	4E-4	2E-2	3E-7	9E-8	7E-7	1E-7	2E-8	8E-6	4E-5	2E-3	9E-2	3E-5	9E-3	1E-2
all	3E-7	5E-7	2E-4	1E-9	1E-6	4E-4	1E-6	7E-7	1E-5	1E-6	5E-6	6E-4	6E-8	2E-7	1E-9

	DC			rho			IDT			LBV			DXfam		
	test1	test2	test3	test1	test2	test3	test1	test2	test3	test1	test2	test3	test1	test2	test3
HC+rho	5E-3	8E-3	1E-2	5E-16	2E-15	1E-16	2E-3	5E-3	1E-2	2E-3	3E-3	1E-2	1E-1	2E-1	2E-1
HC+rho+MW	1E-14	1E-3	7E-3	2E-17	2E-12	4E-6	7E-4	4E-3	4E-3	2E-4	1E-3	7E-3	3E-5	1E-1	2E-1
HC+rho+CN	1E-13	1E-3	2E-2	9E-15	7E-14	4E-16	7E-4	2E-3	2E-3	2E-4	2E-4	2E-3	3E-5	2E-2	1E-1
HC+rho+mu	7E-17	1E-3	3E-2	1E-17	1E-12	1E-14	7E-4	4E-4	9E-3	2E-4	7E-4	2E-2	3E-6	5E-2	3E-1
HC+rho+YSI	2E-12	4E-4	2E-2	4E-14	4E-13	7E-14	7E-4	5E-4	2E-3	2E-4	3E-4	1E-3	2E-4	4E-2	6E-2
HC+rho+DC	8E-16	4E-13	4E-4	2E-17	2E-16	1E-4	7E-4	4E-4	8E-3	2E-4	3E-4	9E-3	8E-6	1E-4	2E-1
HC+rho+IDT	5E-4	2E-3	2E-2	9E-6	1E-6	8E-7	2E-4	7E-5	2E-3	3E-4	5E-4	2E-3	8E-2	1E-1	1E-1
HC+rho+LBV	2E-5	1E-3	4E-2	5E-8	6E-6	3E-7	6E-4	8E-4	1E-2	2E-4	1E-4	7E-5	3E-2	3E-3	9E-2
HC+rho+MW+CN	6E-14	1E-3	8E-3	5E-15	1E-14	2E-5	7E-4	2E-3	2E-3	2E-4	2E-4	2E-3	2E-5	1E-2	1E-1
HC+rho+CN+mu	5E-13	2E-5	1E-2	4E-14	2E-12	2E-6	7E-4	3E-4	2E-3	2E-4	3E-4	2E-3	4E-5	3E-3	1E-1
HC+rho+CN+YSI	3E-17	2E-4	2E-2	5E-19	2E-12	1E-13	7E-4	3E-4	2E-3	2E-4	3E-4	2E-3	3E-6	8E-3	1E-1
HC+rho+CN+DC	7E-14	2E-12	2E-3	7E-15	2E-14	1E-4	7E-4	4E-4	6E-3	2E-4	3E-4	5E-3	3E-5	5E-5	2E-1
HC+rho+CN+IDT	1E-3	6E-4	2E-2	4E-6	1E-6	6E-7	3E-4	2E-4	2E-3	4E-4	5E-4	2E-3	3E-2	2E-2	1E-1
HC+rho+CN+LBV	3E-5	6E-4	5E-2	2E-7	1E-6	4E-4	7E-4	1E-3	2E-3	2E-4	2E-4	5E-4	1E-2	1E-2	8E-2
all	6E-7	9E-6	8E-3	2E-8	1E-6	7E-5	7E-4	4E-4	2E-3	2E-4	3E-4	1E-3	6E-3	2E-3	1E-1

List of symbols and acronyms

Symbol	Meaning
$\bar{0}$	Zero vector
A_i	Antoine's law parameter
B_i	Antoine's law parameter
\bar{c}_i	Point used to build the Kriging model
c_{ij}	j -th component of \bar{c}_i vector
C_i	Antoine's law parameter
CN	Cetane number
CN_i	Cetane number of the species i
CN_{surr}	Cetane number of the surrogate
c_p	Specific heat
DC	Distillation Curve
f, f_{obj}	Objective function
$g_j(\bar{x})$	j -th equality constraint
$H/C, HC$	Hydrogen over carbon ratio
H/C_{surr}	Hydrogen over carbon ratio of the surrogate
h_i	Specific enthalpy
$h_j(\bar{x})$	j -th inequality constraint
IDT	Ignition Delay Time
\dot{j}_j	Diffusive mass flux

Symbol	Meaning
K_i	Partition coefficient
L	Likelihood in Kriging model
LBV	Laminar Burning Velocity
\dot{m}_i	Convective mass flow
MW	Molecular weight
MW_i	Molecular weight of species i
MW_{surr}	Molecular weight of the surrogate
n_{C_i}	Number of carbon atoms in a molecule of species i
n_{H_i}	Number of hydrogen atoms in a molecule of species i
n_i	Number of moles of species i
NP	Number of points used to build the model
N_{points}, N_p	Number of points from which a curve is composed
$N_{species}, N_{sp}$	Number of species present in the mixture
P	Pressure
P_i^o	Vapor pressure of species i
p_{surr}	Property of the surrogate mixture
p_{target}	Property of the target fuel
\mathbb{R}	Set of real numbers
\mathbb{R}^n	Set of n -dimensional real vectors
R^2	Coefficient of determination
\dot{R}_i	Production rate of species i , molar
s_L	Laminar Burning Velocity
$s_{L,i}$	Laminar Burning Velocity of the species i
$s_{L,mix}$	Laminar Burning Velocity of the mixture
T	Temperature
t	Time
U	Internal energy

List of symbols and acronyms

Symbol	Meaning
\mathbf{U}	Cholesky factorization of Ψ
v	Velocity
V	Volume
V_i	Volumetric fraction of species i
w_p	Weight parameter of the property p
\bar{w}	Weights vector
w_i	Weight parameter
x_i	Molar fraction of species i
x_i	Molar fraction of species i in liquid phase
x_j	j -th component of \bar{x} vector
\bar{x}	n -dimensional real vector
$x_{surrogate}$	Molar composition of the surrogate mixture
x_{target}	Molar composition of the target fuel
\bar{y}	Function evaluations vector
y_i	Molar fraction of species i in vapor phase
YSI	Yield Sooting Index
YSI_i	Yield Sooting Index of the species i
YSI_{surr}	Yield Sooting Index of the surrogate
α	Vaporization ratio
α_i	Parameter for viscosity calculation
α_i	Parameter of the polynomial LBV model
β_i	Parameter for viscosity calculation
β_{ij}	Parameter of the polynomial LBV model
γ_i	Parameter for viscosity calculation
γ_{ijk}	Parameter of the polynomial LBV model
δ_i	Parameter for viscosity calculation
Δx^f	Average error on composition (by chemical family)

Symbol	Meaning
ε	Squared relative error
ε_p	Squared relative error on the property p
ϑ, ϑ_j	Parameter of Kriging model
λ	Regularization parameter in Kriging model
λ	Thermal conductivity
μ	Parameter for Kriging likelihood estimation
μ	Viscosity
μ_i	Viscosity of the species i
μ_{surr}	Viscosity of the surrogate
ρ	Density
ρ_i	Density of the species i
ρ_{surr}	Density of the surrogate
$\hat{\sigma}^2$	Parameter for Kriging likelihood estimation
τ	Ignition Delay Time
τ_i	A single IDT, part of an IDT curve
ϕ	Fuel over oxidizer equivalence ratio
ψ	Single Gaussian basis function
Ψ	Matrix of Gaussian basis functions
ω_i	Mass fraction of species i

Bibliography

- (1) British Petroleum. *Statistical Review of World Energy 2020*. URL: <https://www.bp.com/content/dam/bp/business-sites/en/global/corporate/pdfs/energy-economics/statistical-review/bp-stats-review-2020-full-report.pdf>.
- (2) ClimateWatch. *Historical GHG Emissions*. Data from CAIT. URL: <https://www.climatewatchdata.org/ghg-emissions> (visited on 23/06/2021).
- (3) International Energy Agency. *Total final consumption by source, OECD, 1971-2018*. 2018. URL: <https://www.iea.org/data-and-statistics/charts/total-final-consumption-by-source-oecd-1971-2018> (visited on 22/06/2021).
- (4) International Energy Agency. *Final consumption by sector and source, OECD, 2018*. URL: <https://www.iea.org/data-and-statistics/charts/final-consumption-by-sector-and-source-oecd-2018> (visited on 22/06/2021).

- (5) T. Covert, M. Greenstone and C. R. Knittel. “Will We Ever Stop Using Fossil Fuels?” In: *Journal of Economic Perspectives* 30.1 (February 2016), pp. 117–38. DOI: [10.1257/jep.30.1.117](https://doi.org/10.1257/jep.30.1.117).
- (6) European Environment Agency. *Energy statistics - Energy balances*. January 2017. URL: <https://www.eea.europa.eu/data-and-maps/daviz/transport-energy-consumption-eea-5> (visited on 23/06/2021).
- (7) European Environment Agency. *Fuel types and GHG emissions*. 2014. URL: <https://www.eea.europa.eu/media/infographics/fuel-types-and-ghg-emissions/view> (visited on 22/06/2021).
- (8) International Air Transport Association. *IATA Forecast Predicts 8.2 billion Air Travelers in 2037*. URL: <https://www.iata.org/en/pressroom/pr/2018-10-24-02/> (visited on 24/06/2021).
- (9) ASTM. *D1655 - 20d. Standard Specification for Aviation Turbine Fuels*. 2020.
- (10) ASTM. *D6615 - 15a. Standard Specification for Jet B Wide-Cut Aviation Turbine Fuel*. 2019.
- (11) Shell. *Civil Aviation Fuel — Jet Fuel Specifications*. URL: <https://www.shell.com/business-customers/aviation/aviation-fuel/civil-jet-fuel-grades.html> (visited on 23/06/2021).

- (12) Chevron. *Aviation Fuels, Technical Review*. URL: <https://www.chevron.com/-/media/chevron/operations/documents/aviation-tech-review.pdf> (visited on 07/09/2021).
- (13) J. T. Edwards. *Jet Fuel Properties*. Ed. by Air Force Research Laboratory Wright-Patterson AFB United States. 2020. URL: <https://apps.dtic.mil/sti/citations/AD1093317> (visited on 07/09/2021).
- (14) D. D. Das, C. S. McEnally, T. A. Kwan, J. B. Zimmerman, W. J. Cannella, C. J. Mueller and L. D. Pfefferle. “Sooting tendencies of diesel fuels, jet fuels, and their surrogates in diffusion flames”. In: *Fuel* 197 (2017), pp. 445–458. ISSN: 0016-2361. DOI: <https://doi.org/10.1016/j.fuel.2017.01.099>.
- (15) Shell. *Jet Fuel Additives — Aviation & Aircraft Fuel Additives*. URL: <https://www.shell.com/business-customers/aviation/aviation-fuel/aeroshell-performance-additive.html> (visited on 23/06/2021).
- (16) ASTM. *D4054 - 20c. Standard Practice for Evaluation of New Aviation Turbine Fuels and Fuel Additives*. 2020.
- (17) D. Demetryouss. “Metamodel-based optimization for the formulation of jet fuel surrogates”. Politecnico di Milano, 2020.
- (18) URL: <https://www.opensmokepp.polimi.it>.
- (19) A. Cuoci, A. Frassoldati, T. Faravelli and E. Ranzi. “OpenSMOKE++: An object-oriented framework for the numerical modeling of reactive systems with detailed kinetic mechanisms”. In: *Computer Phys-*

-
- ics Communications* 192 (2015), pp. 237–264. ISSN: 0010-4655. DOI: <https://doi.org/10.1016/j.cpc.2015.02.014>.
- (20) CRECK Modeling Group. *Kinetic mechanisms for hydrocarbon fuels*. URL: <http://creckmodeling.chem.polimi.it/menu-kinetics> (visited on 23/06/2021).
- (21) J. Kendall and K. P. Monroe. “The viscosity of liquids. II. The viscosity-composition curve for ideal liquid mixtures.1”. In: *Journal of the American Chemical Society* 39.9 (1917), pp. 1787–1802. DOI: [10.1021/ja02254a001](https://doi.org/10.1021/ja02254a001).
- (22) H.A. Kooijman and R. Taylor. *The ChemSep Book*. H.A. Kooijman and R. Taylor, 2000. ISBN: 9783831110681. URL: <https://books.google.it/books?id=huAWHtZ0dCEC>.
- (23) J. H. Holland. “Genetic Algorithms”. In: *Scientific American* 267.1 (1992), pp. 66–73. ISSN: 00368733, 19467087. URL: <http://www.jstor.org/stable/24939139>.
- (24) J. Kennedy and R. Eberhart. “Particle swarm optimization”. In: *Proceedings of ICNN’95 - International Conference on Neural Networks*. Vol. 4. 1995, 1942–1948 vol.4. DOI: [10.1109/ICNN.1995.488968](https://doi.org/10.1109/ICNN.1995.488968).
- (25) C. Audet and J. E. Dennis. “Analysis of Generalized Pattern Searches”. In: *SIAM Journal on Optimization* 13.3 (2002), pp. 889–903. DOI: [10.1137/S1052623400378742](https://doi.org/10.1137/S1052623400378742).

- (26) K. Deep, K. P. Singh, M.L. Kansal and C. Mohan. “A real coded genetic algorithm for solving integer and mixed integer optimization problems”. In: *Applied Mathematics and Computation* 212.2 (2009), pp. 505–518. ISSN: 0096-3003. DOI: [10.1016/j.amc.2009.02.044](https://doi.org/10.1016/j.amc.2009.02.044).
- (27) R. Byrd, J. Gilbert and J. Nocedal. “A trust region method based on interior point techniques for nonlinear programming”. In: *Math. Program.* 89 (2000), pp. 149–185. DOI: [10.1007/PL00011391](https://doi.org/10.1007/PL00011391).
- (28) *fsolve documentation*. URL: <https://it.mathworks.com/help/optim/ug/fsolve.html> (visited on 26/05/2021).
- (29) K. Narayanaswamy, H. Pitsch and P. Pepiot. “A component library framework for deriving kinetic mechanisms for multi-component fuel surrogates: Application for jet fuel surrogates”. In: *Combustion and Flame* 165 (2016), pp. 288–309. ISSN: 0010-2180. DOI: <https://doi.org/10.1016/j.combustflame.2015.12.013>. URL: <https://www.sciencedirect.com/science/article/pii/S0010218015004563>.
- (30) CRECK Modeling Group. *Kinetic mechanisms for hydrocarbon fuels*. URL: http://creckmodeling.chem.polimi.it/images/site/kinetic_mechanisms/version1412/POLIMI_1412.zip (visited on 22/05/2021).
- (31) *rmoutliers documentation*. URL: <https://it.mathworks.com/help/matlab/ref/rmoutliers.html> (visited on 27/05/2021).

-
- (32) A. Sóbester A. I. J. Forrester and A. J. Keane. *Engineering Design via Surrogate Modelling*. Ed. by John Wiley and Sons Ltd. 2008. DOI: [10.1002/9780470770801](https://doi.org/10.1002/9780470770801).
- (33) *Optimization Codes for design and analysis of computational and physical experiments*. URL: <https://www.wiley.com/go/forrester> (visited on 27/05/2021).
- (34) L. Sileghem, J. Vancoillie, J. Demuynck, J. Galle and S. Verhelst. “Alternative Fuels for Spark-Ignition Engines: Mixing Rules for the Laminar Burning Velocity of Gasoline–Alcohol Blends”. In: *Energy & Fuels* 26.8 (2012), pp. 4721–4727. DOI: [10.1021/ef300393h](https://doi.org/10.1021/ef300393h).
- (35) S. Dooley, S. Hee Won, M. Chaos, J. Heyne, Y. Ju, F. L. Dryer, K. Kumar, C.-J. Sung, H. Wang, M. A. Oehlschlaeger, R. J. Santoro and T. A. Litzinger. “A jet fuel surrogate formulated by real fuel properties”. In: *Combustion and Flame* 157.12 (2010), pp. 2333–2339. ISSN: 0010-2180. DOI: <https://doi.org/10.1016/j.combustflame.2010.07.001>.
- (36) T. Bruno, M. Huber, A. Laesecke, E. Lemmon, M. McLinden, S. Outcalt, R. Perkins, B. Smith and J. Widegren. *Thermodynamic, Transport, and Chemical Properties of Reference JP-8*. en. 2010-07-14 2010. URL: https://tsapps.nist.gov/publication/get_pdf.cfm?pub_id=904848.

- (37) D. D. Das, C. S. McEnally, T. A. Kwan, J. B. Zimmerman, W. J. Cannella, C. J. Mueller and L. D. Pfefferle. “Sooting tendencies of diesel fuels, jet fuels, and their surrogates in diffusion flames”. In: *Fuel* 197 (2017), pp. 445–458. ISSN: 0016-2361. DOI: <https://doi.org/10.1016/j.fuel.2017.01.099>.
- (38) C. Saggese, A. V. Singh, X. Xue, C. Chu, M. Reza Kholghy, T. Zhang, J. Camacho, J. Giaccai, J. H. Miller, M. J. Thomson, C.-J. Sung and H. Wang. “The distillation curve and sooting propensity of a typical jet fuel”. In: *Fuel* 235 (2019), pp. 350–362. ISSN: 0016-2361. DOI: <https://doi.org/10.1016/j.fuel.2018.07.099>.
- (39) CRECK Modeling Group. *Detailed mechanisms*. March 2020. URL: <http://creckmodeling.chem.polimi.it/menu-kinetics/menu-kinetics-detailed-mechanisms> (visited on 28/07/2021).
- (40) S. Dooley, F. Dryer, S. Hee Won and T. Farouk. “Reduced Kinetic Models for the Combustion of Jet Propulsion Fuels”. In: *51st AIAA Aerospace Sciences Meeting including the New Horizons Forum and Aerospace Exposition*. DOI: [10.2514/6.2013-158](https://doi.org/10.2514/6.2013-158).
- (41) D. Kim, J. Martz and A. Violi. “A surrogate for emulating the physical and chemical properties of conventional jet fuel”. In: *Combustion and Flame* 161.6 (2014), pp. 1489–1498. ISSN: 0010-2180. DOI: <https://doi.org/10.1016/j.combustflame.2013.12.015>.

- (42) T. Edwards. *Reference Jet Fuels for Combustion Testing*. 2017. URL: https://www.caafi.org/news/pdf/Edwards_AIAA-2017-0146_Reference_Jet_Fuels.pdf (visited on 27/07/2021).
- (43) A.R. De Toni, M. Werler, R.M. Hartmann, L.R. Cancino, R. Schießl, M. Fikri, C. Schulz, A.A.M. Oliveira, E.J. Oliveira and M.I. Rocha. “Ignition delay times of Jet A-1 fuel: Measurements in a high-pressure shock tube and a rapid compression machine”. In: *Proceedings of the Combustion Institute* 36.3 (2017), pp. 3695–3703. ISSN: 1540-7489. DOI: <https://doi.org/10.1016/j.proci.2016.07.024>.
- (44) V. Vukadinovic, P. Habisreuther and N. Zarzalis. “Influence of pressure and temperature on laminar burning velocity and Markstein number of kerosene Jet A-1: Experimental and numerical study”. In: *Fuel* 111 (2013), pp. 401–410. ISSN: 0016-2361. DOI: <https://doi.org/10.1016/j.fuel.2013.03.076>.